

Supporting Information

Pyrrolidinyl peptide nucleic acid with α/β -peptide backbone: A conformationally constrained PNA with unusual hybridization properties

Chotima Vilaivan, Choladda Srisuwannaket, Cheeraporn Ananthanawat, Chaturong Suparpprom, Junji Kawakami, Yoshie Yamaguchi, Yuko Tanaka, and Tirayut Vilaivan*

N-tert-Butoxycarbonyl-*cis*-4-hydroxy-L-proline diphenylmethyl ester (**1a**)

N-tert-Butoxycarbonyl-*trans*-4-hydroxy-L-proline diphenylmethyl ester (1.21 g, 3.0 mmol), triphenylphosphine (1.00 g, 3.6 mmol) and formic acid (0.12 mL, 3.0 mmol) were dissolved in dry THF (10 mL) in a dried 100 mL round bottom flask equipped with a magnetic bar and then cool down to 0 °C in an ice-salt bath. The solution was stirred under nitrogen balloon and DIAD (0.70 mL, 3.6 mmol) was added dropwise over 15 min and the reaction mixture was allowed to stir at 30 °C for 8 h. Chromatographic purification afforded the *cis*-4-formate ester intermediate (1.78 g, quantitative yield). ¹H NMR (400 MHz, CDCl₃, TMS): δ =1.32 and 1.51 (2×s, 9H; CH₃ Boc rotamers), 2.32–2.39 [m, 1H; 1×CH₂(3')], 2.45–2.50 [m, 1H; 1×CH₂(3')], 3.52–3.79 [m, 2H; CH₂(5')], 4.53–4.68 [2×m, 1H; CH(2')], 5.25–5.33 [m, 1H; CH(4')], 6.95 and 6.99 (2×s, 1H; CHPh₂ rotamers), 7.24–7.37 (m, 10H, Ar CH); ¹³C NMR (100 MHz, CDCl₃, TMS): δ =28.1 and 28.4 (CH₃ Boc rotamers), 35.4 and 36.3 [CH₂(3') rotamers], 52.0 and 52.3 [CH₂(5') rotamers], 57.6 and 57.9 [CH(2') rotamers], 71.4 and 72.5 [CH(4') rotamers], 77.6 and 77.7 (CCH₃ Boc rotamers), 80.4 and 80.5 (CH Dpm rotamers), 127.1–128.5 (CH Ar Dpm rotamers) 139.7 (C Dpm), 153.6 and 153.9 (CO Boc rotamers), 159.9 (CHO) 170.5 and 170.7 (CO ester rotamers).

A portion of this formate ester (1.21 g, 3.0 mmol) was dissolved in methanol (10 mL) and concentrated aqueous ammonia solution (1 mL) was added. After 1 h, the ammonolysis was completed as indicated by TLC analysis. The solvent was removed under reduced pressure and the oily residue was purified by column chromatography on silica gel using ethyl acetate:hexanes (1:2) as eluent to give **1a** as a clear viscous oil (1.78 g, quantitative yield). $[\alpha]_D^{25}$ =−14.6 (*c*=3.28 in CHCl₃); ¹H NMR (400 MHz, CDCl₃, TMS) (Figure S3): δ =1.27 and 1.49 (2×s, 9H, CH₃ Boc), 2.09 [t, *J*=7.6 Hz, 1H; 1×CH₂(3')], 2.28–2.42 [m, 1H; 1×CH₂(3')], 3.56–3.70 [m, 2H; CH₂(5')], 4.31–4.38 [br, 1H; CH(4')], 4.45 and 4.57 [2×m, 1H; CH(2')], 6.91 and 6.99 (2×s, 1H; CHPh₂ rotamers), 7.29–7.37 (m, 10H, Ar CH); ¹³C NMR (100 MHz, CDCl₃, TMS) (Figure S4): δ =28.0 and 28.3 (CH₃ Boc rotamers), 37.7 and 38.6 [CH₂(3') rotamers], 55.2 and 55.6 [CH₂(5') rotamers], 58.1 [CH(2')], 69.9 and 70.8 [CH(4') rotamers], 77.9 and 78.4 (CCH₃ Boc rotamers), 80.2 and 80.4 (CH Dpm rotamers) 126.9–128.5 (CH Ar Dpm), 139.5 (C Dpm), 153.8 and 154.3 (CO Boc rotamers), 173.3 and 173.6 (CO ester rotamers); elemental analysis calcd (%) for C₂₃H₂₇NO₅: C 69.50, H 6.85, N 3.52; found: C 69.51, H 6.68, N 3.51.

N-tert-Butoxycarbonyl-(2'*S*,4'*R*)-(N³-benzoylthymine-1-yl)-proline diphenyl methyl ester (**2a**)

N-tert-Butoxycarbonyl-*cis*-4-hydroxy-L-proline diphenylmethyl ester (**1a**) (1.21 g, 3.04 mmol), triphenylphosphine (1.23 g, 4.56 mmol) and N³-benzoylthymine (1.05

mL, 4.56 mmol) were dissolved in dry THF (20 mL) and then cool down to 0 °C in an ice-salt bath. The solution was stirred under nitrogen balloon and diisopropyl azodicarboxylate (DIAD) (0.88 mL, 4.56 mmol) was added dropwise over a period of 15 min. The reaction mixture was allowed to stir at 30 °C for 8 h. The solvent was removed under reduced pressure and the residue was purified by column chromatography through silica gel using ethyl acetate:hexanes (1:2) as eluent to give **2a** as a clear viscous oil (1.12 g, 60% yield). m.p.=103–105 °C; $[\alpha]_D^{25} = -36.0$ ($c=1.06$ in CHCl_3); $^1\text{H NMR}$ (400 MHz, CDCl_3 , TMS) (Figure S5): $\delta=1.31$ and 1.50 (2xs, 9H, CH_3 Boc rotamers), 1.98 (s, 3H; CH_3 Thymine), 2.32 – 2.44 [m, 1H; $1\times\text{CH}_2(3')$], 2.53 – 2.66 [m, 1H; $1\times\text{CH}_2(3')$], 3.61 – 3.82 [$2\times$ m, 1H; $1\times\text{CH}_2(5')$], 3.92 – 4.00 [m, 1H; $1\times\text{CH}_2(5')$], 4.57 – 4.72 [$2\times$ m, 1H; $\text{CH}(4')$], 5.11 – 5.19 [m, 1H; $\text{CH}(2')$], 6.91 and 6.96 (2xs, 1H; CHPh_2), 7.05 [s, 1H; C(6)H Thymine], 7.29 – 7.37 [m, 10H, Ar Dpm], 7.52 [t, $J=7.7$ Hz, 2H; $\text{CH}(3,5)$ Bz], 7.68 [t, $J=7.3$ Hz, 1H; $\text{CH}(4)$ Bz], 7.94 [d, $J=7.5$ Hz, 2H; $\text{CH}(2,6)$ Bz]; $^{13}\text{C NMR}$ (100 MHz, CDCl_3 , TMS) (Figure S6): $\delta=12.7$ (CH_3 Thymine), 28.0 and 28.3 (CH_3 Boc rotamers), 33.4 and 35.0 [$\text{CH}_2(3')$ rotamers], 49.1 and 49.6 [$\text{CH}_2(5')$ rotamers], 53.8 and 54.4 [$\text{CH}(4')$ rotamers], 57.8 and 58.0 [$\text{CH}(2')$ rotamers], 77.9 and 78.1 (CCH_3 Boc rotamers), 81.1 and 81.2 (CH Dpm rotamers), 111.6 ($\text{C}5$ Thymine), 126.8 – 128.6 (CH Ar Dpm), 129.2 ($\text{C}4$ Bz), 130.4 ($\text{C}2$ and $\text{C}6$ Bz), 131.3 ($\text{C}3$ and $\text{C}5$ Bz), 135.2 and 136.2 ($\text{C}1$ Bz), 149.6 (C Dpm), 153.4 and 153.8 ($\text{C}2$ Thymine), 162.5 ($\text{C}4$ Thymine), 168.9 (CO Boc), 170.8 (CO ester); elemental analysis calcd (%) for $\text{C}_{35}\text{H}_{35}\text{N}_3\text{O}_7$: C 68.95, H, 5.79, N, 6.89; found: C 68.97, H, 5.80, N 6.89.

***N*-Fluoren-9-ylmethoxycarbonyl-(2'*S*,4'*R*)-(thymine-1-yl)-proline (3a)**

N-tert-Butoxycarbonyl-(2'*S*,4'*R*)-4-(*N*³-benzoylthymine-1-yl)proline diphenylmethyl ester (**2a**) (0.80 g, 1.32 mmol) was treated with 10% anisole in trifluoroacetic acid (5 mL) at room temperature overnight. The solvents were removed under a stream of nitrogen. After washing with diethyl ether, the residue was dissolved in a minimum amount of 1:1 aqueous acetonitrile and was treated with solid NaHCO_3 until pH=8 followed by addition of FmocOSu (0.49 g, 1.45 mmol). After stirring at room temperature overnight, the reaction mixture was extracted with diethyl ether and the aqueous phase acidified with conc HCl. The titled compound was obtained as a white solid after filtration and washing with water (0.33 g, 53% yield). $[\alpha]_D^{25} = +1.80$ ($c=1.00$ in DMF); $^1\text{H NMR}$ (400 MHz, $\text{DMSO}-d_6$, TMS) (Figure S7): $\delta=1.80$ (s, 3H; CH_3 Thymine), 2.20 – 2.33 [m, 1H; $1\times\text{CH}_2(3')$], 2.59 – 2.74 [m, 1H; $1\times\text{CH}_2(3')$], 3.46 – 3.50 [m, 1H; $1\times\text{CH}_2(5')$], 3.73 – 3.83 [m, 1H; $1\times\text{CH}_2(5')$], 4.24 – 4.31 (m, 3H; CH and CH_2 Fmoc), 4.41 – 4.57 [$2\times$ m, 1H; $\text{CH}(2')$ rotamers], 5.04 – 5.12 [m, 1H; $\text{CH}(4')$], 7.31 – 7.36 (m, 2H; CH Fmoc), 7.41 – 7.46 (m, 2H; Ar CH Fmoc), 7.62 [s, 1H; C(6)H Thymine], 7.59 – 7.68 (m, 2H; Ar CH Fmoc), 7.90 – 7.92 (m, 2H; Ar CH Fmoc) 11.36 , 11.39 (2xs, 1H; COOH rotamers); $^{13}\text{C NMR}$ (100 MHz, $\text{DMSO}-d_6$, TMS) (Figure S8): $\delta=12.6$ (CH_3 Thymine), 32.6 and 33.7 [$\text{CH}_2(3')$ rotamers], 46.9 and 47.0 (CH Fmoc rotamers), 49.2 and 49.4 [$\text{CH}_2(5')$ rotamers], 52.2 and 53.2 [$\text{CH}(4')$ rotamers], 57.9 and 58.1 [$\text{CH}(2')$ rotamers], 67.3 and 67.6 [CH_2 Fmoc rotamers], 109.9 ($\text{C}5$ Thymine), 120.5 and 120.6 (CH Ar Fmoc rotamers), 125.5 – 125.7 (CH Ar Fmoc), 127.6 (CH Ar Fmoc), 128.1 (CH Ar Fmoc), 138.0 and 138.1 [$\text{C}(6)\text{H}$ Thymine rotamers], 141.1 (C Ar Fmoc), 144.0 (C Ar Fmoc), 151.3 ($\text{C}2$ Thymine), 153.9 and 154.2 (CO Fmoc rotamers), 164.1 ($\text{C}4$ Thymine), 173.5 and 173.8

(COOH rotamers); HRMS (FAB⁺): m/z calcd for C₂₅H₂₄O₆N₃: 462.1665 [M+H]⁺; found: 462.1646.

***N*-Fluoren-9-ylmethoxycarbonyl-(2'*R*,4'*S*)-(thymine-1-yl)-proline (3b)**

Synthesis of the titled compound was accomplished in the same way as described for compound **3a** above starting from the known intermediate *N*-*tert*-butoxycarbonyl-(2'*R*,4'*S*)-4-(*N*³-benzoylthymine-1-yl)proline diphenylmethyl ester (**2b**)² (1.57 g, 2.57 mmol) to afford the compound **3b** as a white solid (0.97 g, 82% yield). [α]_D²⁵ = -2.90 (*c* = 1.00 in DMF) ¹H NMR (400 MHz, DMSO-*d*₆, TMS) (Figure S9): δ = 1.80 (s, 3H; CH₃ Thymine), 2.21–2.33 [m, 1H; 1×CH₂(3')], 2.60–2.75 [m, 1H; 1×CH₂(3')], 3.45–3.53 [m, 1H; 1×CH₂(5')], 3.74–3.83 [m, 1H; 1×CH₂(5')], 4.18–4.41 (m, 3H; CH Fmoc and CH₂ Fmoc), 4.41 and 4.57 [2×m, 1H; CH(2') rotamers], 5.05–5.12 [m, 1H; CH(4')], 7.32–7.36 (m, 2H; CH Ar Fmoc), 7.40–7.46 (m, 2H; CH Ar Fmoc), 7.62 [m, 1H; C(6)H Thymine], 7.65–7.67 (m, 2H; CH Ar Fmoc), 7.89–7.92 (m, 2H; CH Ar Fmoc), 11.36 and 11.39 (2×s, 1H; CO₂H rotamers); ¹³C NMR (100 MHz, DMSO-*d*₆, TMS) (Figure S10): δ = 12.6 (CH₃ Thymine), 32.6 and 33.7 [CH₂(3') rotamers], 46.9 (CH Fmoc), 49.2 and 49.4 [CH₂(5') rotamers], 52.2 and 53.2 [CH(4') rotamers], 57.8 and 58.0 [CH(2') rotamers], 67.3 and 67.6 (CH₂ Fmoc rotamers), 109.9 (C5 Thymine), 120.5 (CH Ar Fmoc), 125.6 (CH Ar Fmoc), 127.6 (CH Ar Fmoc), 128.1 (CH Ar Fmoc), 138.0 [C(6)H Thymine], 141.1 (CH Ar Fmoc), 144.0 and 144.1 (C Ar Fmoc rotamers), 151.3 (C2 Thymine), 153.9 and 154.2 (CO Fmoc rotamers), 164.1 (C4 Thymine), 173.5 and 173.8 (COOH rotamers); HRMS (FAB⁺): m/z calcd for C₂₅H₂₄O₆N₃: 462.1665 [M+H]⁺; found: 462.1665.

***N*-Fluoren-9-ylmethoxycarbonyl-(2'*S*,4'*S*)-(thymine-1-yl)-proline (3c)**

Synthesis of the titled compound was accomplished in the same way as described for compound **3a** above starting from the known intermediate *N*-*tert*-butoxycarbonyl-(2'*S*,4'*S*)-4-(*N*³-benzoylthymine-1-yl)proline diphenylmethyl ester (**2c**)² (1.10 g, 1.80 mmol) to afford the compound **3c** as a white solid (0.59 g, 72% yield). [α]_D²⁵ = -9.80 (*c* = 1.00 in DMF); ¹H NMR (400 MHz, DMSO-*d*₆, TMS) (Figure S11): δ = 1.79 (s, 3H; CH₃ Thymine), 2.15–2.31 [m, 1H; 1×CH₂(3')], 2.60–2.77 [2×m, 1H; 1×CH₂(3')], 3.47–3.55 [m, 1H; 1×CH₂(5')], 3.86–3.93 [m, 1H; 1×CH₂(5')], 4.18–4.50 [2×m, 1H; CH(2')], 4.24–4.34 (m, 3H; CH₂ Fmoc and CH Fmoc), 4.94–5.00 [m, 1H; CH(4')], 7.35 (t *J* = 7.2 Hz, 2H; CH Ar Fmoc), 7.43 (t *J* = 7.6 Hz, 2H; CH Ar Fmoc), 7.61 [s, 1H; C(6)H Thymine], 7.69 (d, *J* = 7.3 Hz, 2H; CH Ar Fmoc), 7.90 (d *J* = 7.4 Hz, 2H; CH Ar Fmoc), 11.36 (s, 1H; CO₂H); ¹³C NMR (100 MHz, DMSO-*d*₆, TMS) (Figure S12): δ = 12.5 (CH₃ Thymine), 33.1 and 34.3 [CH₂(3') rotamers], 47.0 and 47.1 [CH Fmoc rotamers], 48.8 and 49.4 [CH₂(5') rotamers], 52.7 and 53.2 [CH(4') rotamers], 57.4 and 57.8 [CH(2') rotamers], 67.4 and 67.7 (CH₂ Fmoc rotamers), 109.5 and 109.6 (C5 Thymine rotamers), 120.6 (CH Ar Fmoc), 125.6 (CH Ar Fmoc), 125.8 (CH Ar Fmoc), 127.6 (CH Ar Fmoc), 128.2 (CH Ar Fmoc), 138.3 [C(6)H Thymine], 141.1 (C Ar Fmoc), 144.1 (C Ar Fmoc), 151.4 (C2 Thymine), 154.4 (CO Fmoc), 164.2 (C4 Thymine), 173.1 and 173.6 (COOH rotamers); HRMS (FAB⁺): m/z calcd for C₂₅H₂₄O₆N₃: 462.1665 [M+H]⁺; found: 462.1648.

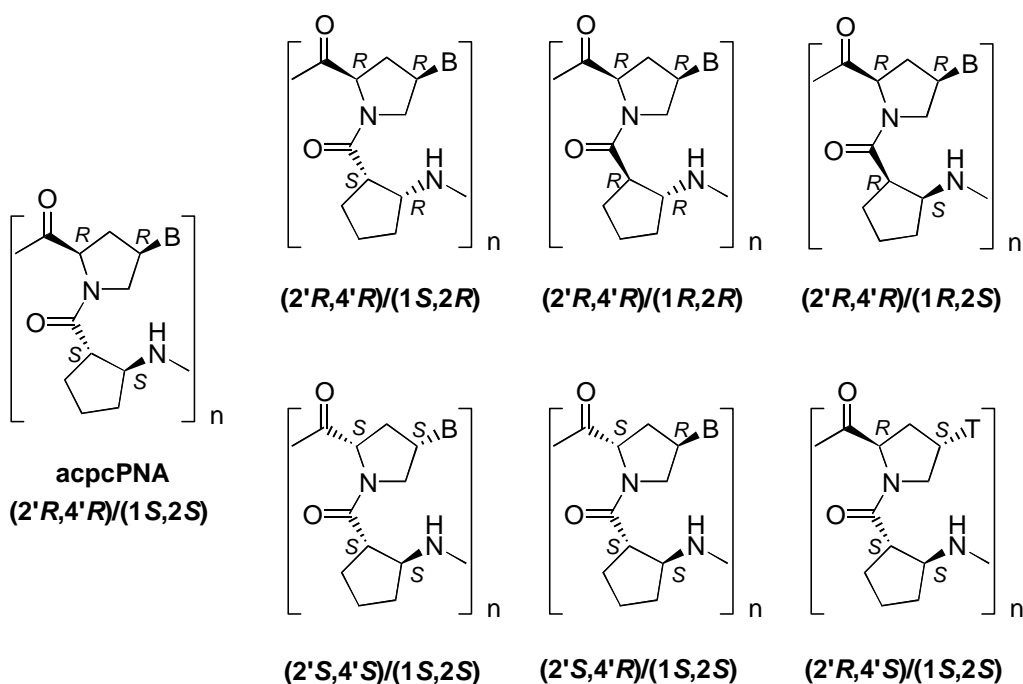


Figure S1. Structures of stereoisomers of acpcPNA that have been evaluated for DNA binding properties in this work. All PNA sequences have B=thymine, $n=5$ and C-terminal lysine capped. The N-termini were either free [(2'R,4'R)/(1S,2S), (2'R,4'R)/(1S,2R), (2'R,4'R)/(1R,2R) and (2'R,4'R)/(1R,2S)] or acetylated [(2'S,4'S)/(1S,2S), (2'S,4'R)/(1S,2S), (2'R,4'R)/(1S,2S) and (2'R,4'S)/(1S,2S)].

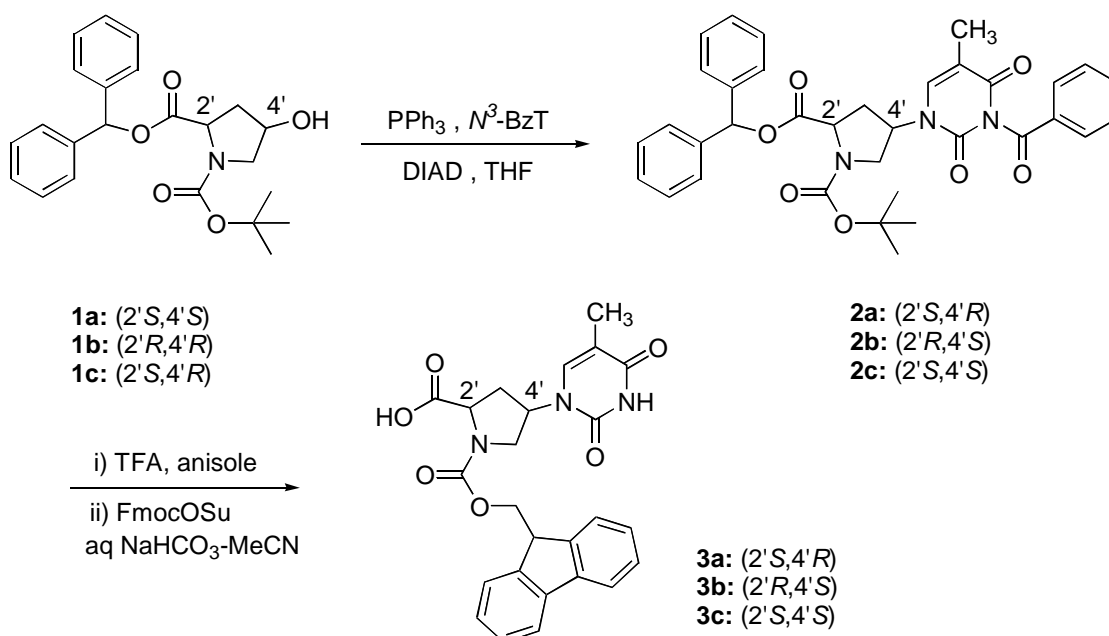


Figure S2. Synthesis of pyrrolidine PNA monomers carrying thymine base (T) with different configurations on the proline ring. Syntheses and characterization data of the (2'R,4'R)-T, as well as C, G and A monomers have already been reported.¹

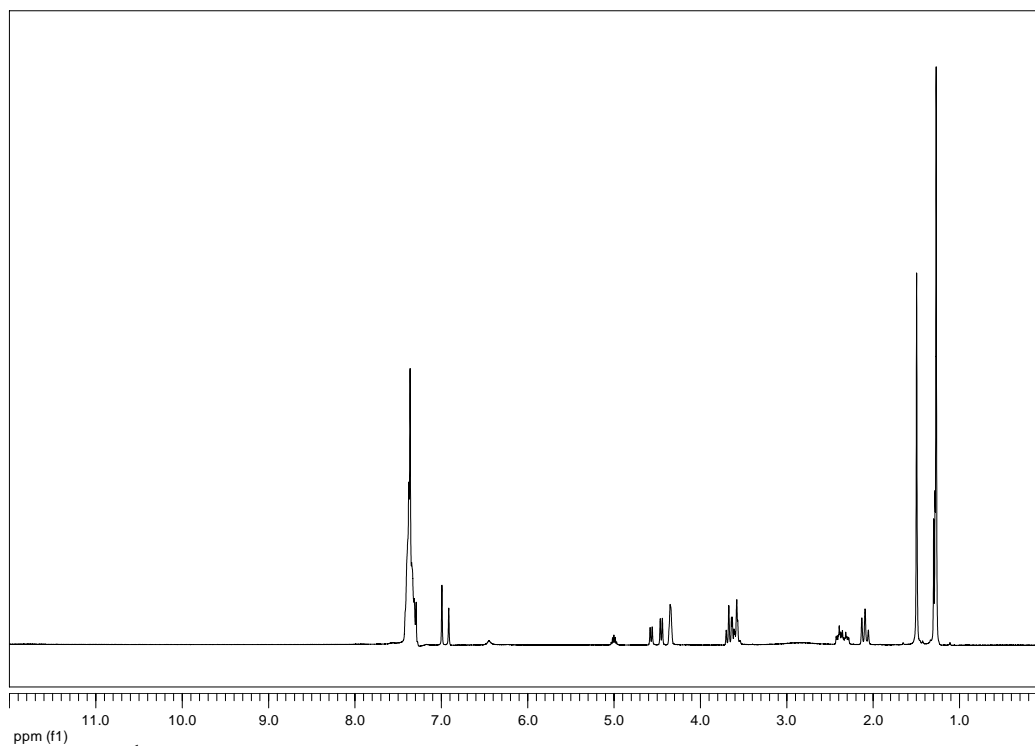


Figure S3. ¹H NMR spectrum (400 MHz, CDCl₃) of *N*-*tert*-Butoxycarbonyl-*cis*-4-hydroxy-L-proline diphenylmethyl ester (**1a**)

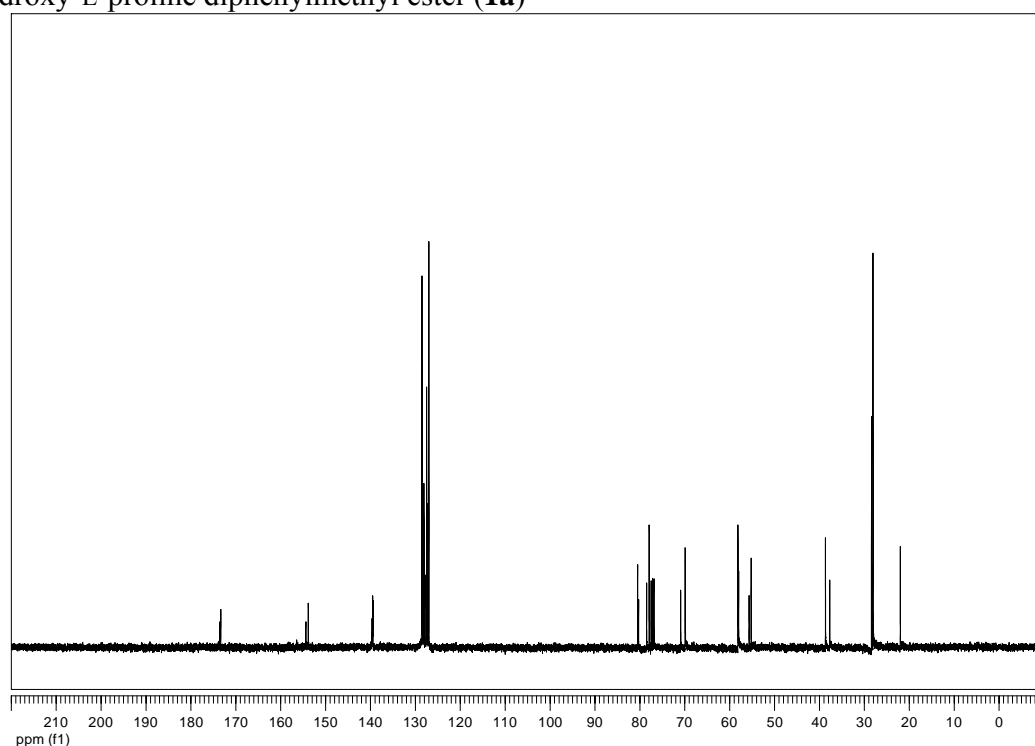


Figure S4. ¹³C NMR spectrum (100 MHz, CDCl₃) of *N*-*tert*-Butoxycarbonyl-*cis*-4-hydroxy-L-proline diphenylmethyl ester (**1a**)

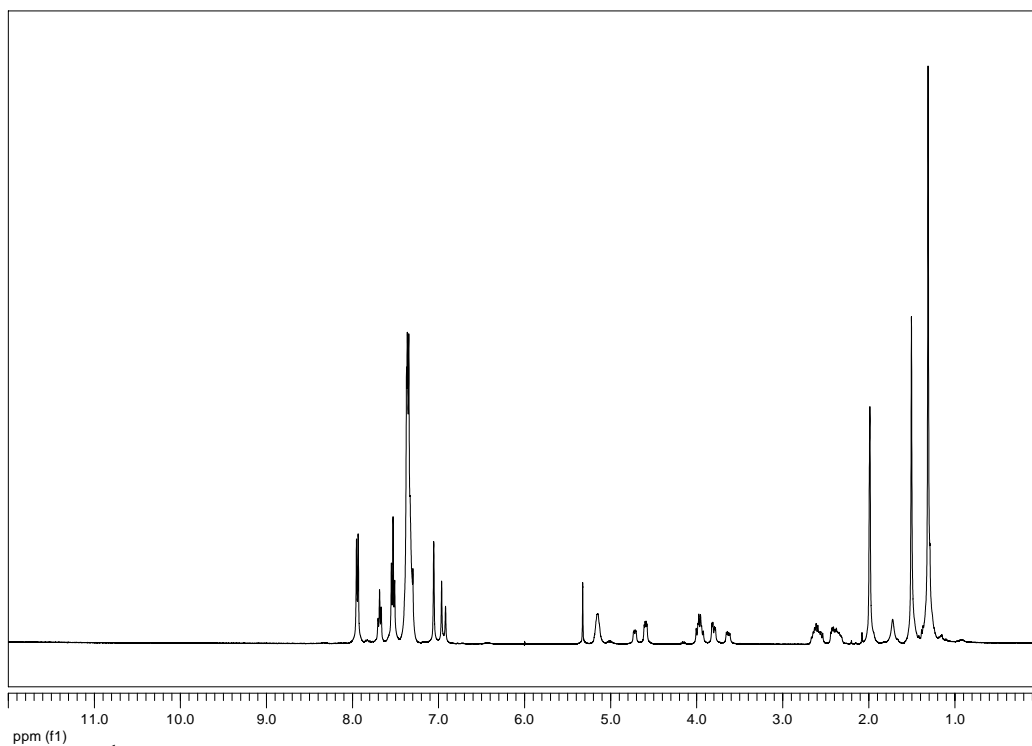


Figure S5. ¹H NMR spectrum (400 MHz, CDCl₃) of *N*-*tert*-Butoxycarbonyl-(2'*S*,4'*R*)-(N³-benzoylthymine-1-yl)-proline diphenyl methyl ester (**2a**)

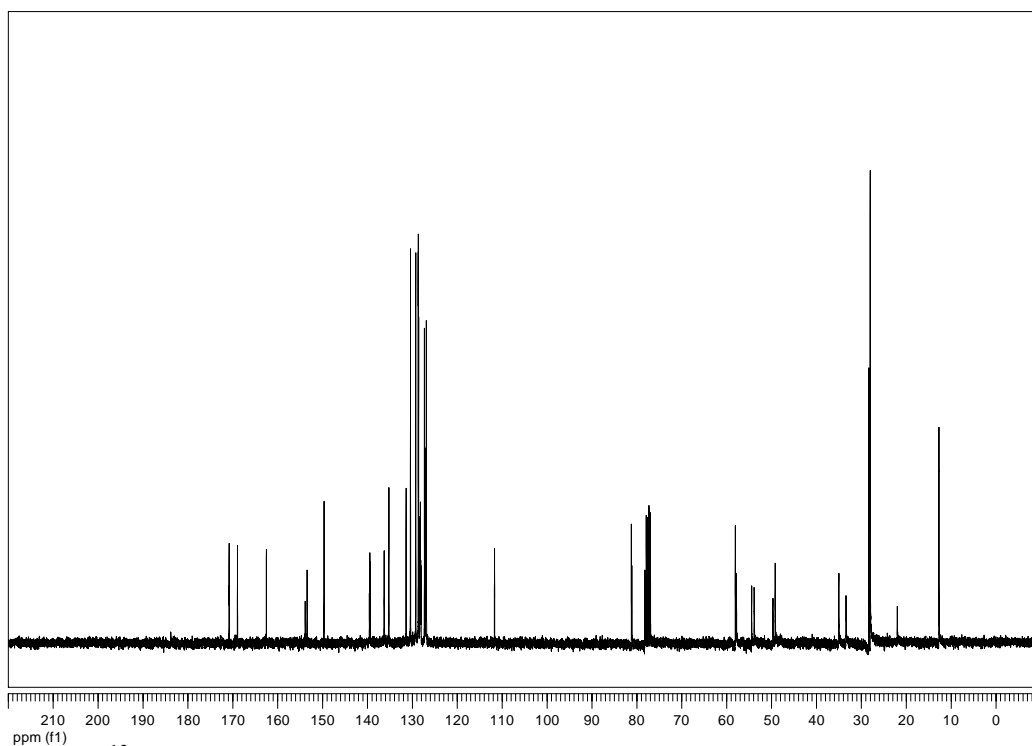


Figure S6. ¹³C NMR spectrum (100 MHz, CDCl₃) of *N*-*tert*-Butoxycarbonyl-(2'*S*,4'*R*)-(N³-benzoylthymine-1-yl)-proline diphenyl methyl ester (**2a**)

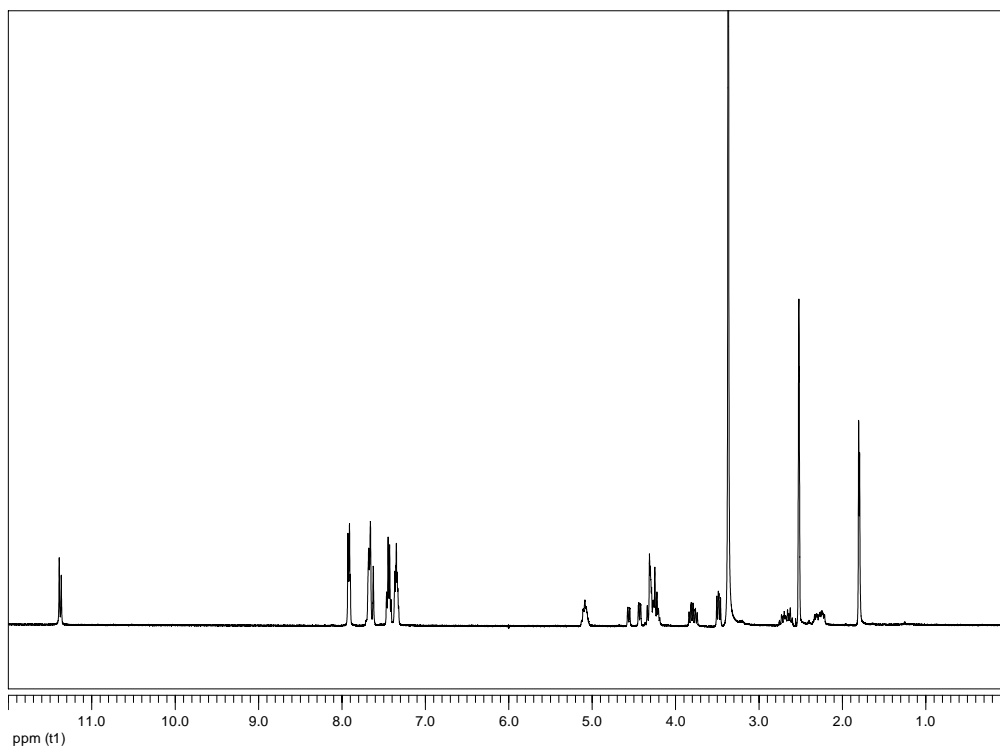


Figure S7. ¹H NMR spectrum (400 MHz, DMSO-*d*₆) of *N*-Fluoren-9-ylmethoxycarbonyl-(2'*S*,4'*R*)-(thymine-1-yl)-proline (**3a**)

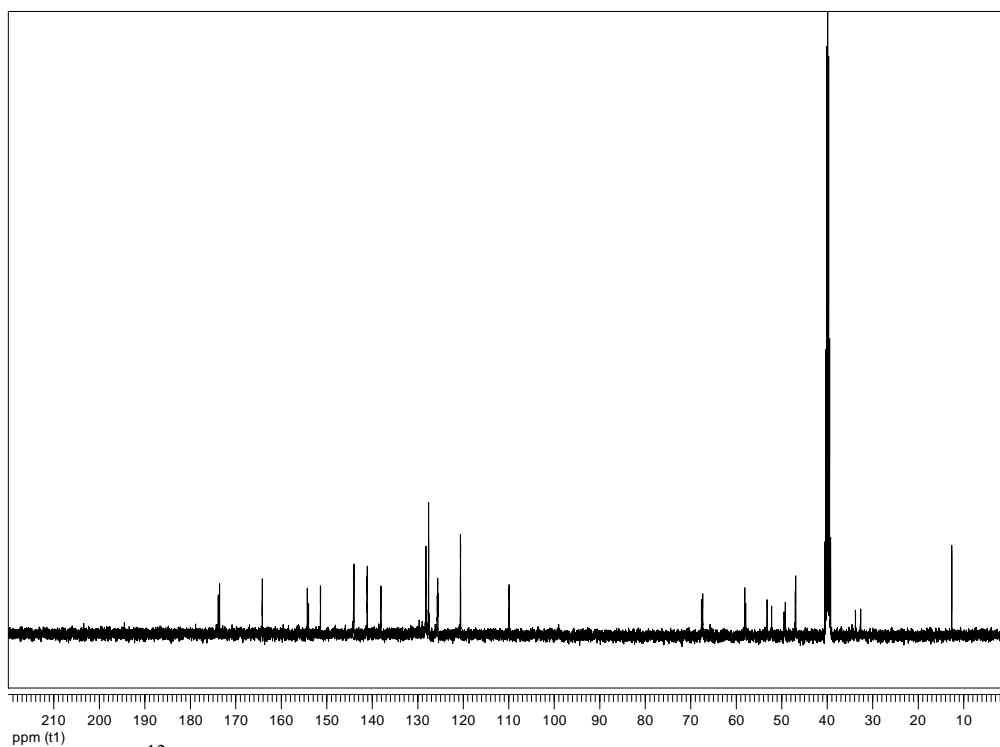


Figure S8. ¹³C NMR spectrum (100 MHz, DMSO-*d*₆) of *N*-Fluoren-9-ylmethoxycarbonyl-(2'*S*,4'*R*)-(thymine-1-yl)-proline (**3a**)

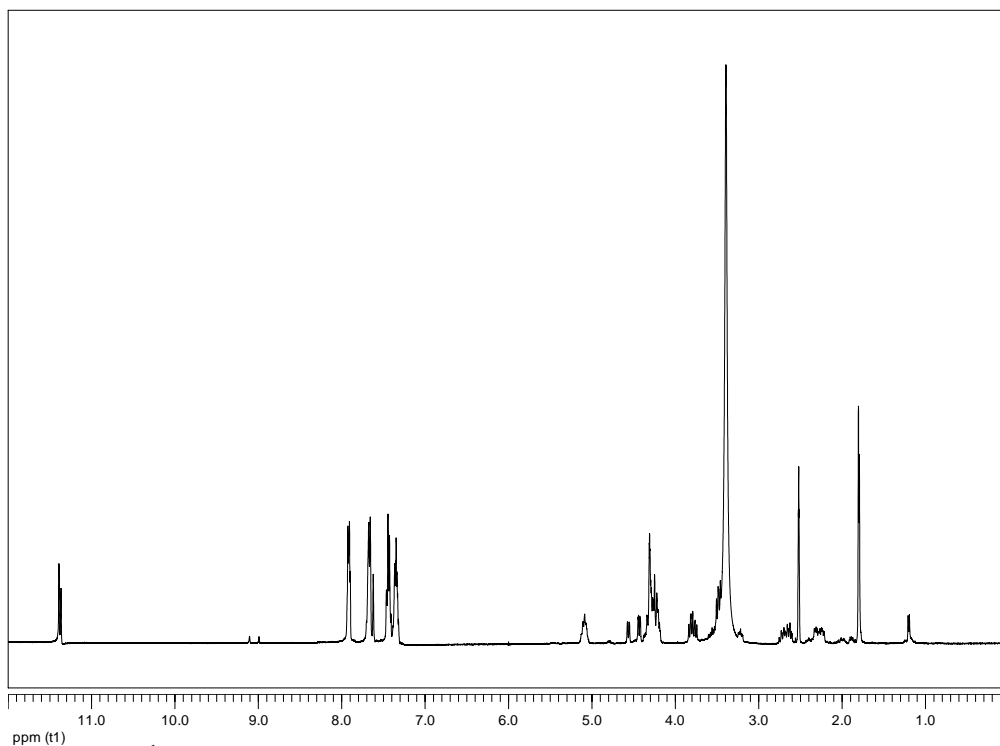


Figure S9. ^1H NMR spectrum (400 MHz, $\text{DMSO-}d_6$) of *N*-Fluoren-9-ylmethoxycarbonyl-(2'*R*,4'*S*)-(thymine-1-yl)-proline (**3b**)

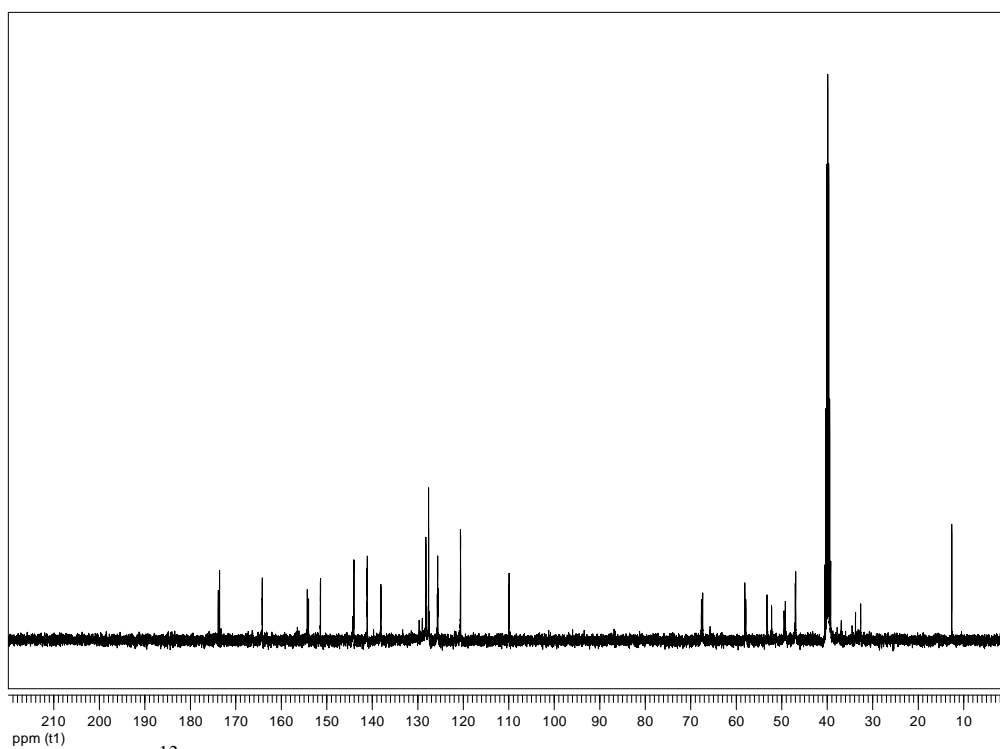


Figure S10. ^{13}C NMR spectrum (100 MHz, $\text{DMSO-}d_6$) of *N*-Fluoren-9-ylmethoxycarbonyl-(2'*R*,4'*S*)-(thymine-1-yl)-proline (**3b**)

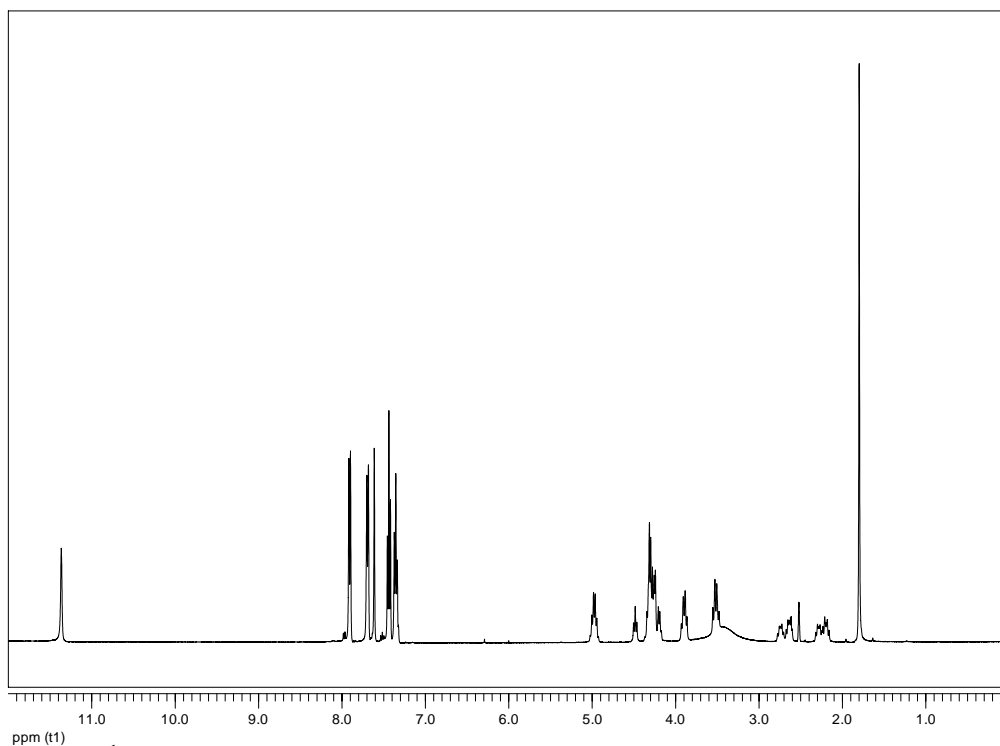


Figure S11. ¹H NMR spectrum (400 MHz, DMSO-*d*₆) of *N*-Fluoren-9-ylmethoxycarbonyl-(2'*S*,4'*S*)-(thymine-1-yl)-proline (**3c**)

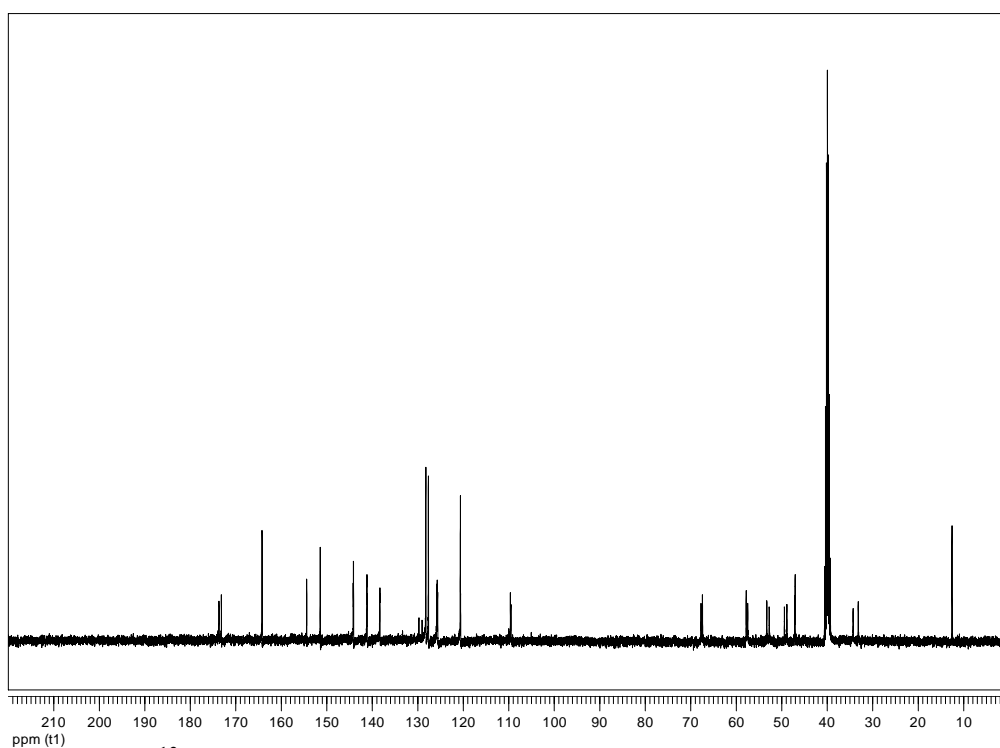


Figure S12. ¹³C NMR spectrum (100 MHz, DMSO-*d*₆) of *N*-Fluoren-9-ylmethoxycarbonyl-(2'*S*,4'*S*)-(thymine-1-yl)-proline (**3c**)

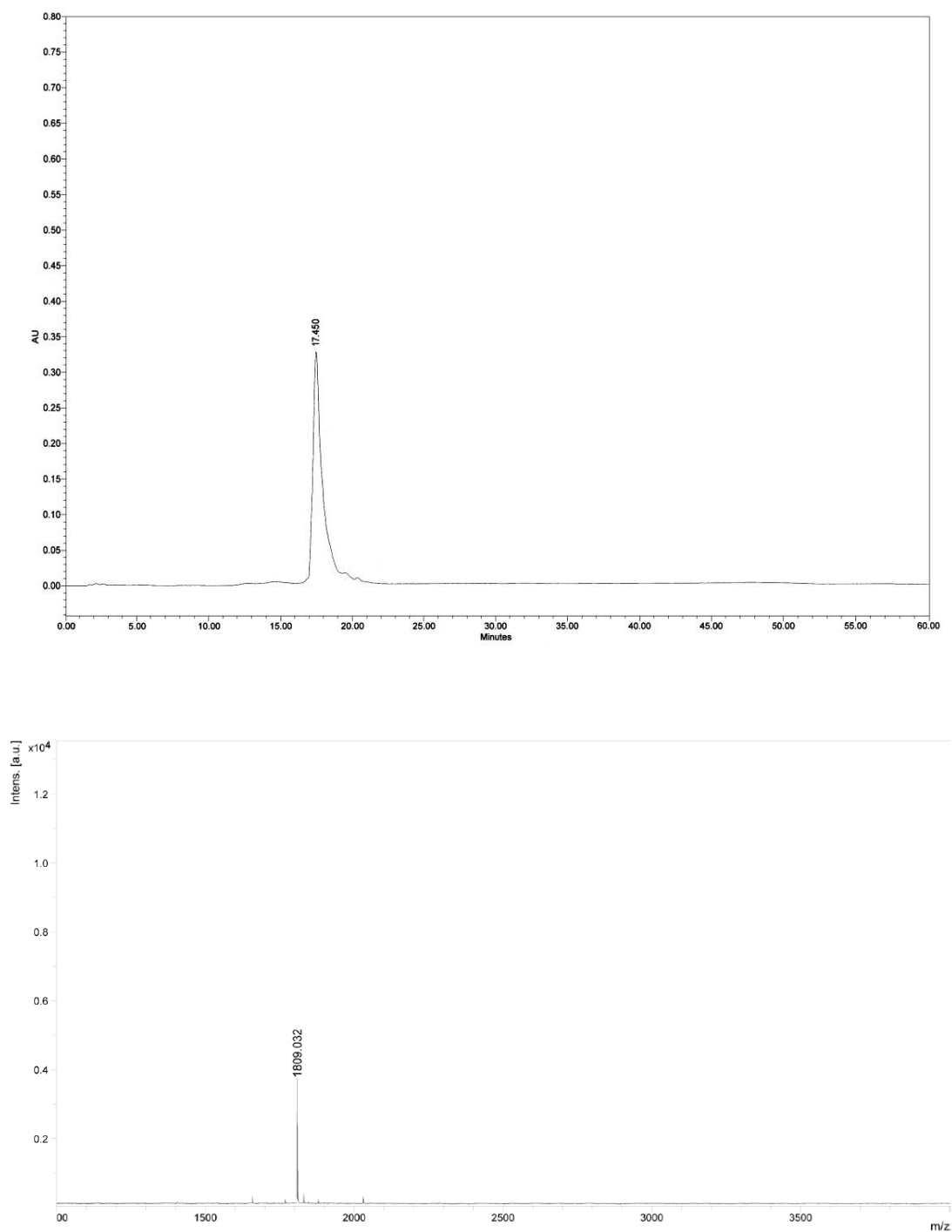


Figure S13. HPLC chromatogram (top) and MALDI-TOF mass spectrum (bottom) of (2'*R*,4'*R*)-pro/(1*S*,2*S*)-acpcPNA H-T₅-LysNH₂ (CCA matrix, Reflectron mode) (calcd for [M+H]⁺: *m/z*=1806.7)

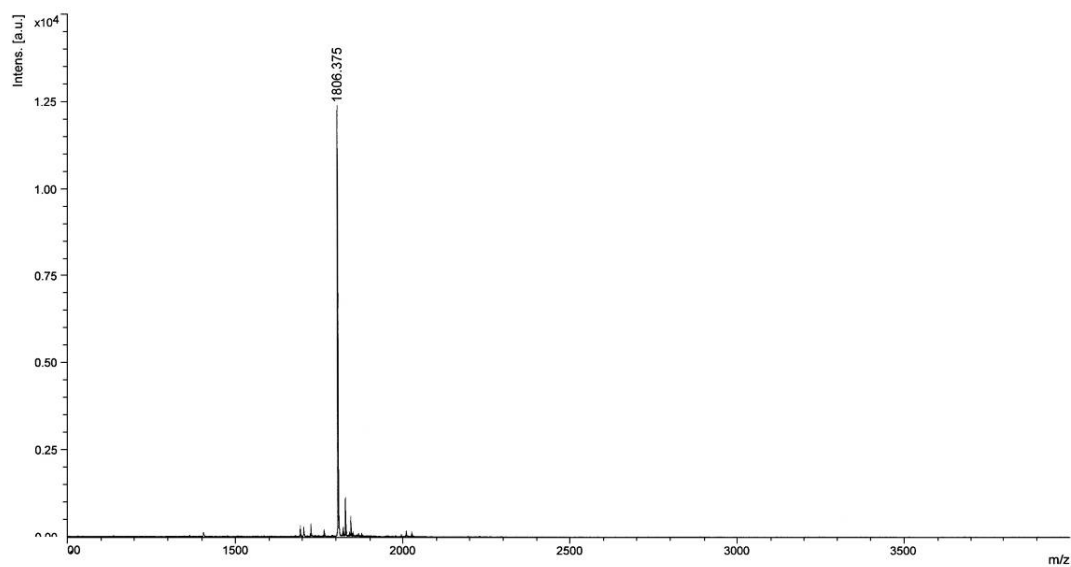
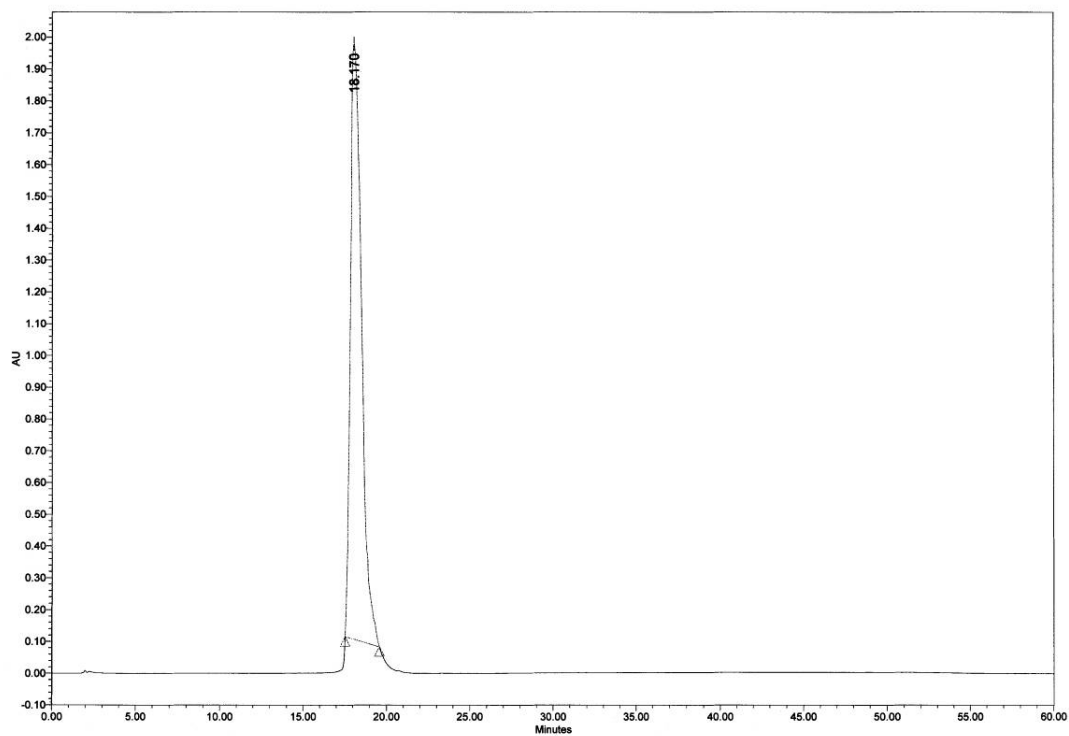


Figure S14. HPLC chromatogram (top) and MALDI-TOF mass spectrum (bottom) of (2'*R*,4'*R*)-pro/(1*S*,2*R*)-acpcPNA H-T₅-LysNH₂ (CCA matrix, Reflectron mode) (calcd for $[M+H]^+$: $m/z=1806.7$)

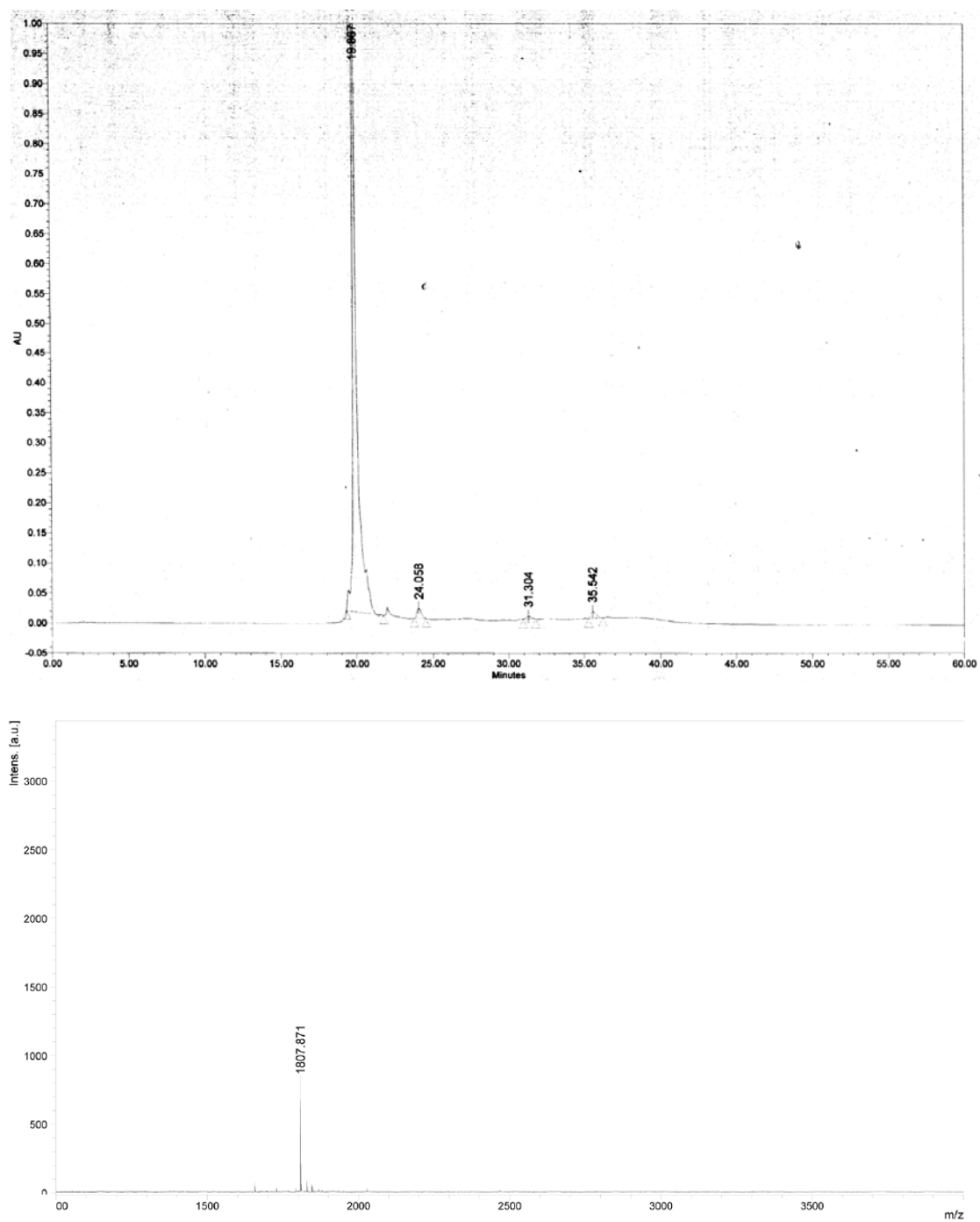


Figure S15. HPLC chromatogram (top) and MALDI-TOF mass spectrum (bottom) of (2'*R*,4'*R*)-pro/(1*R*,2*R*)-acpcPNA H-T₅-LysNH₂ (CCA matrix, Reflectron mode) (calcd for [M+H]⁺: *m/z*=1806.7)

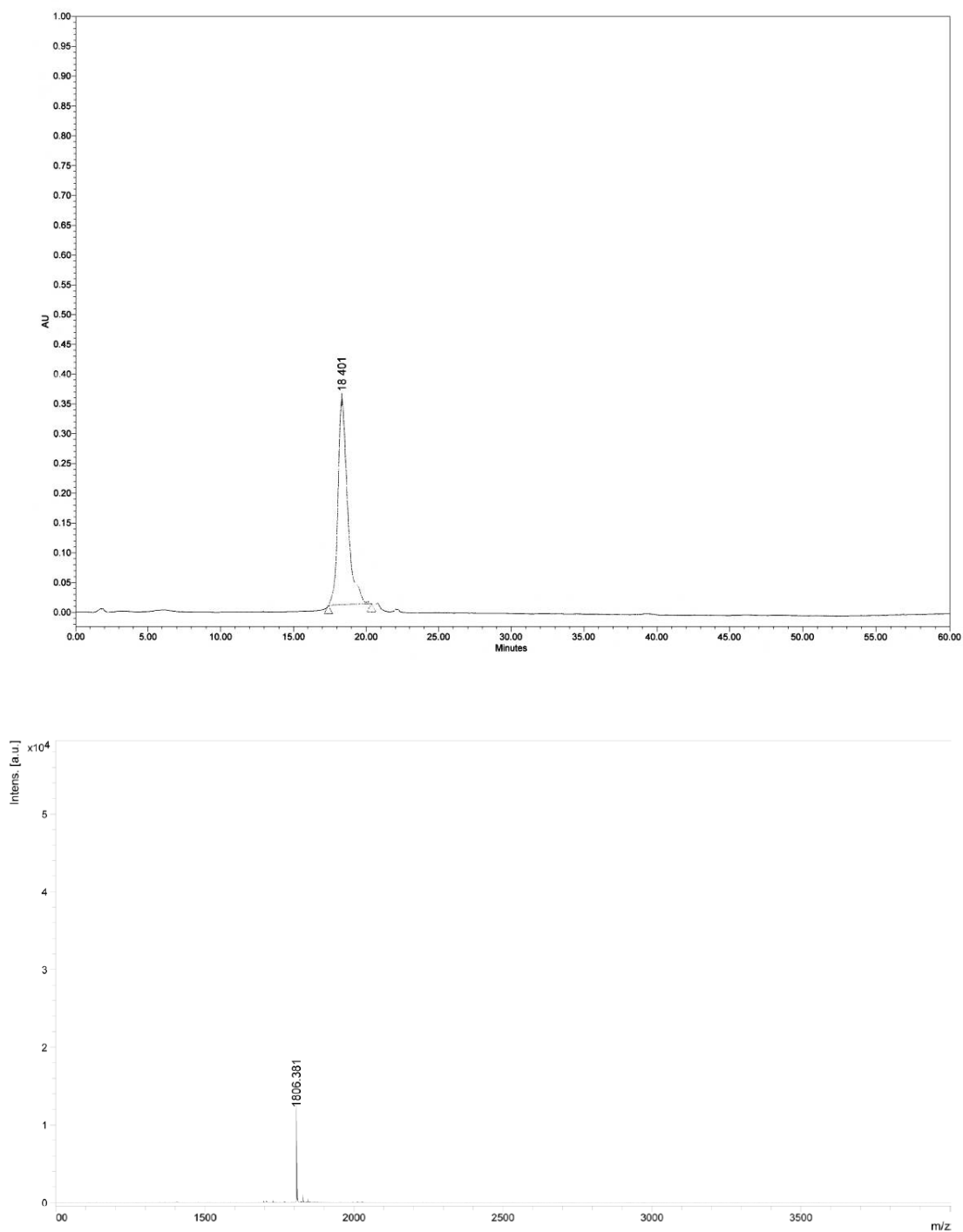


Figure S16. HPLC chromatogram (top) and MALDI-TOF mass spectrum (bottom) of (2'*R*,4'*R*)-pro/(1*R*,2*S*)-acpcPNA H-T₅-LysNH₂ (CCA matrix, Reflectron mode) (calcd for [M+H]⁺: *m/z*=1806.7)

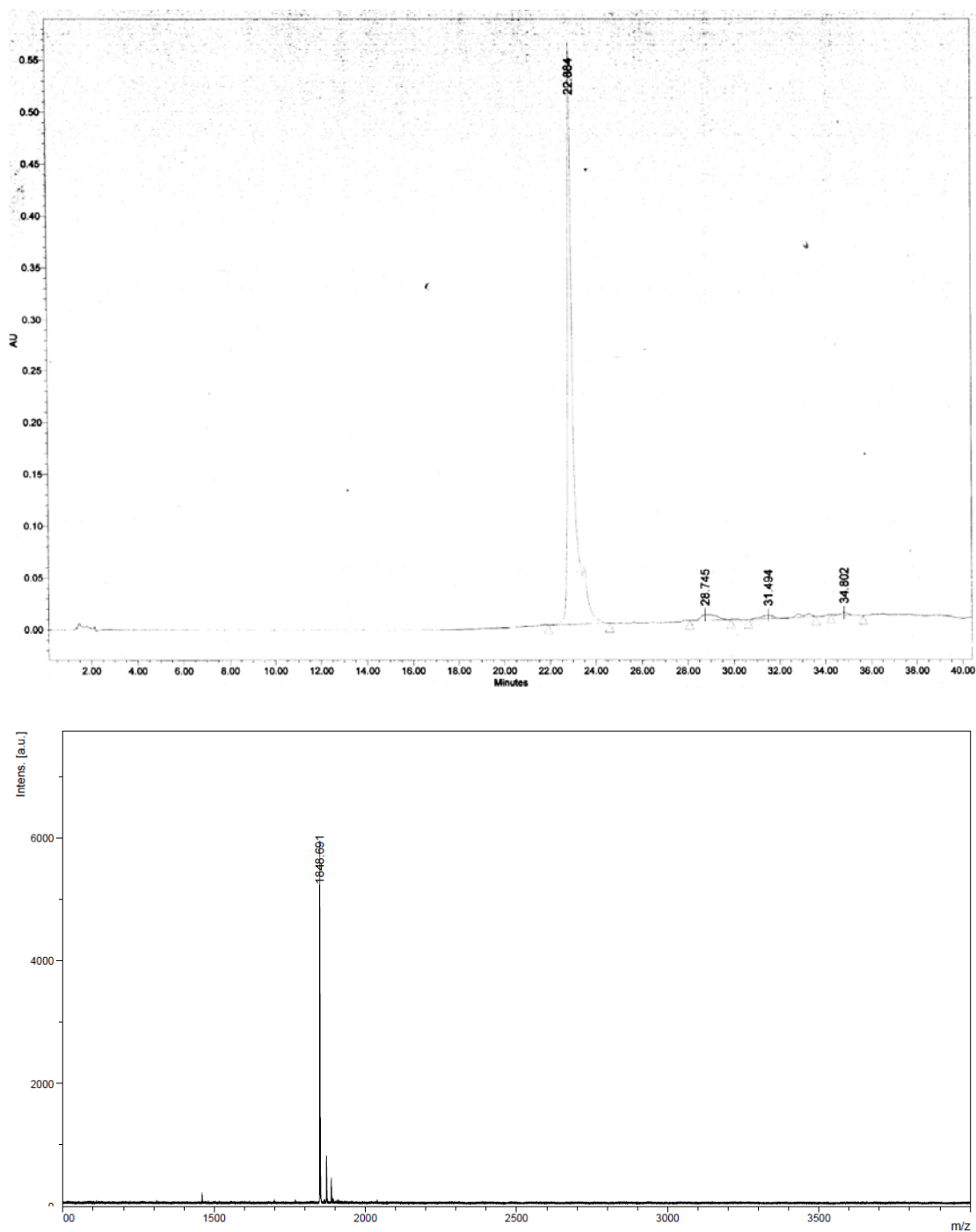


Figure S17. HPLC chromatogram (top) and MALDI-TOF mass spectrum (bottom) of (2'S,4'S)-pro/(1S,2S)-acpcPNA Ac-T₅-LysNH₂ (CCA matrix, Reflectron mode) (calcd for [M+H]⁺: $m/z=1848.9$)

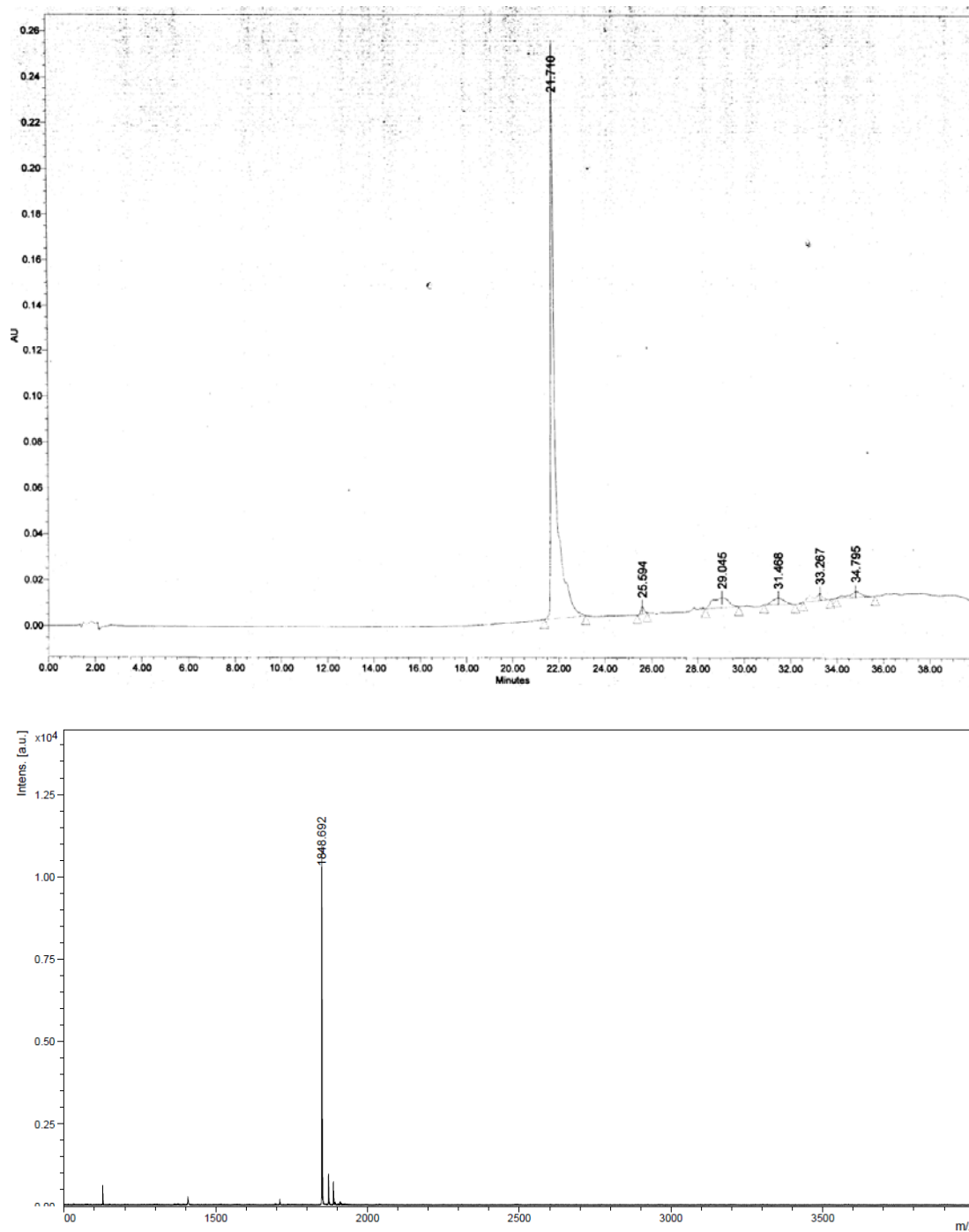


Figure S18. HPLC chromatogram (top) and MALDI-TOF mass spectrum (bottom) of (2'*R*,4'*S*)-pro/(1*S*,2*S*)-acpcPNA Ac-T₅-LysNH₂ (**T5**) (CCA matrix, Reflectron mode) (calcd for $[M+H]^+$: $m/z=1848.9$)

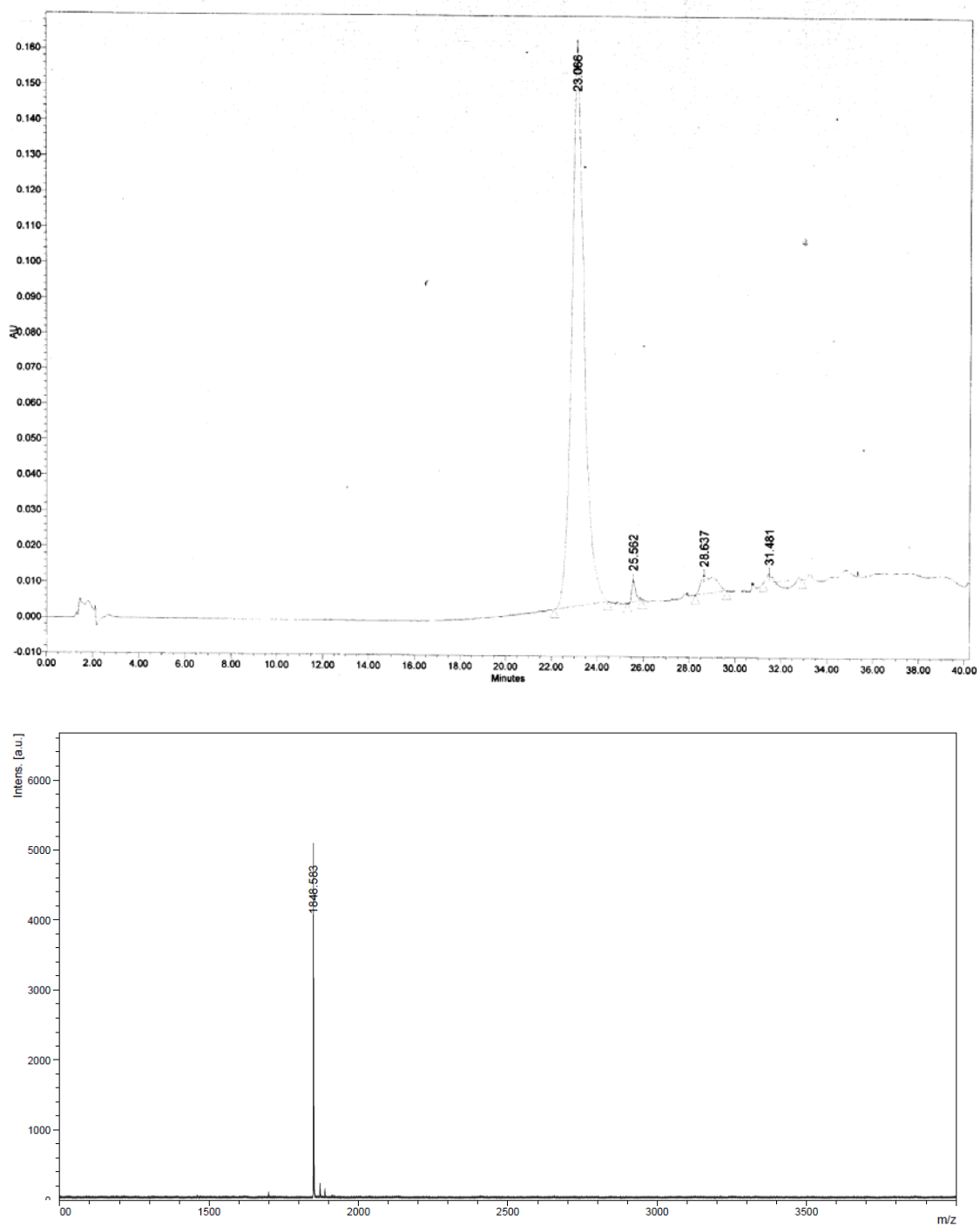


Figure S19. HPLC chromatogram (top) and MALDI-TOF mass spectrum (bottom) of (2'*S*,4'*R*)-pro/(1*S*,2*S*)-acpcPNA Ac-T₅-LysNH₂ (CCA matrix, Reflectron mode) (calcd for $[M+H]^+$: $m/z=1848.9$)

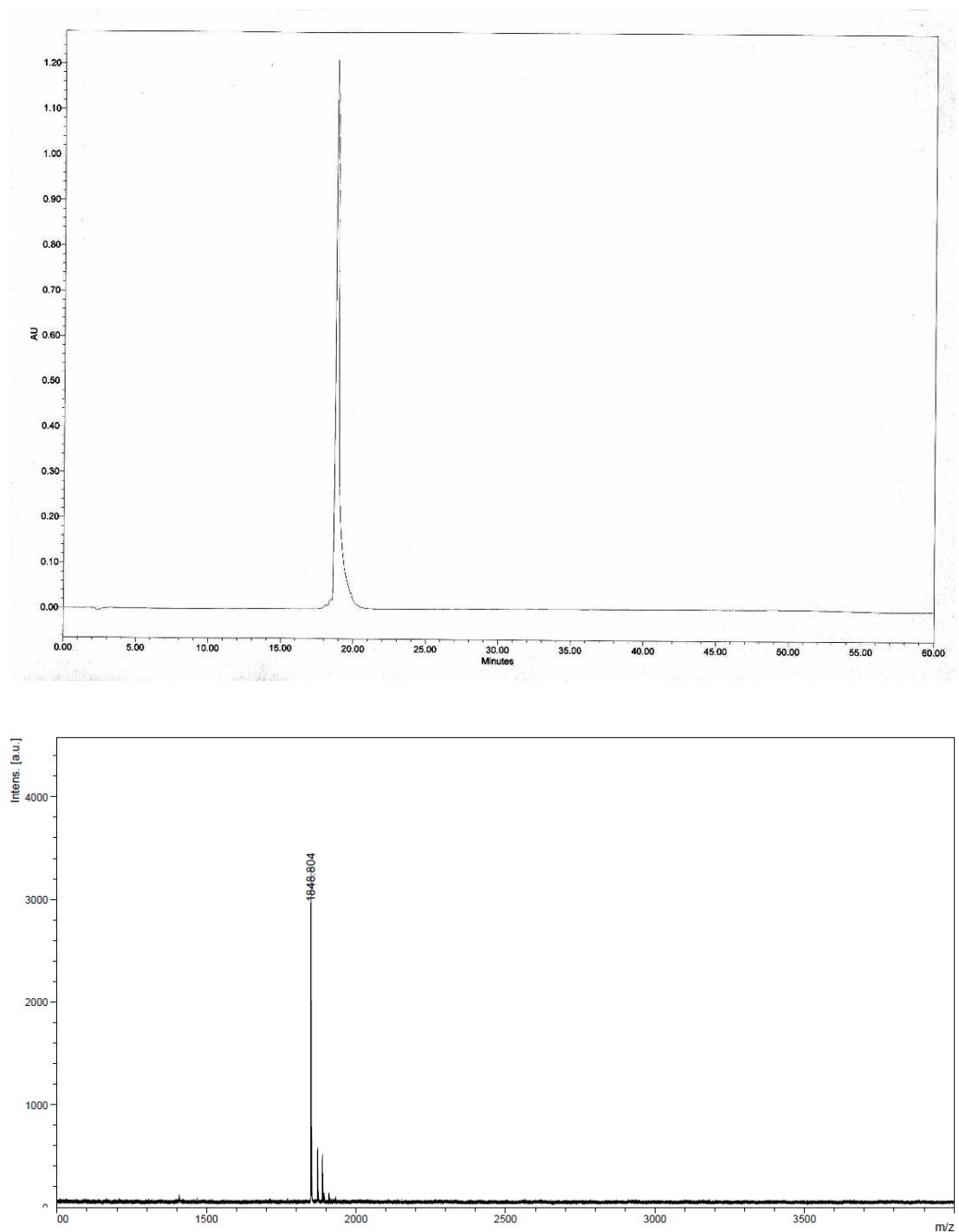


Figure S20. HPLC chromatogram (top) and MALDI-TOF mass spectrum (bottom) of (2'*R*,4'*R*)-pro/(1*S*,2*S*)-acpc Ac-T₅-LysNH₂ (**T5**) (CCA matrix, Reflectron mode) (calcd $M \cdot H^+$: $m/z=1848.9$)

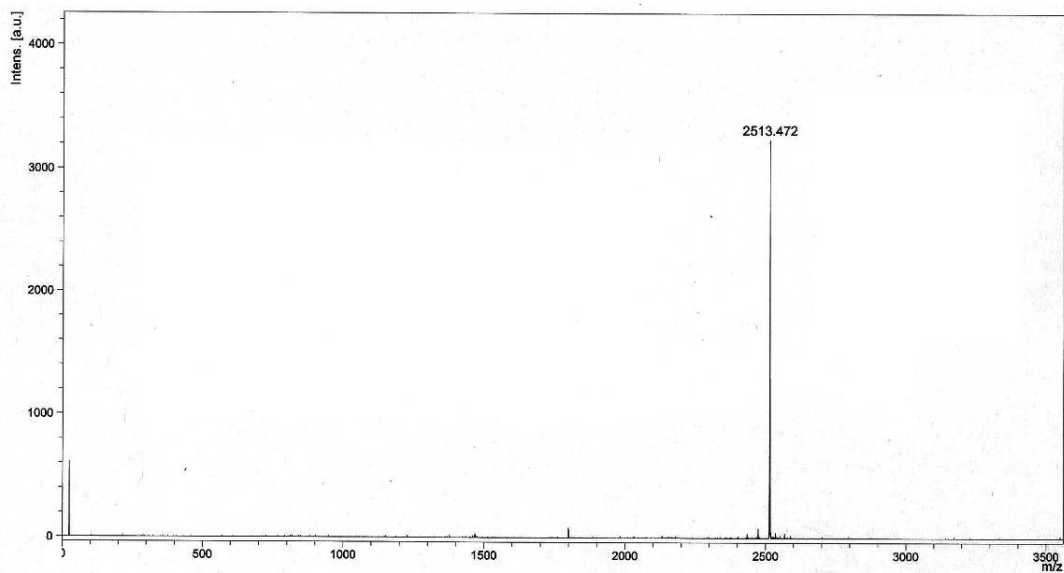
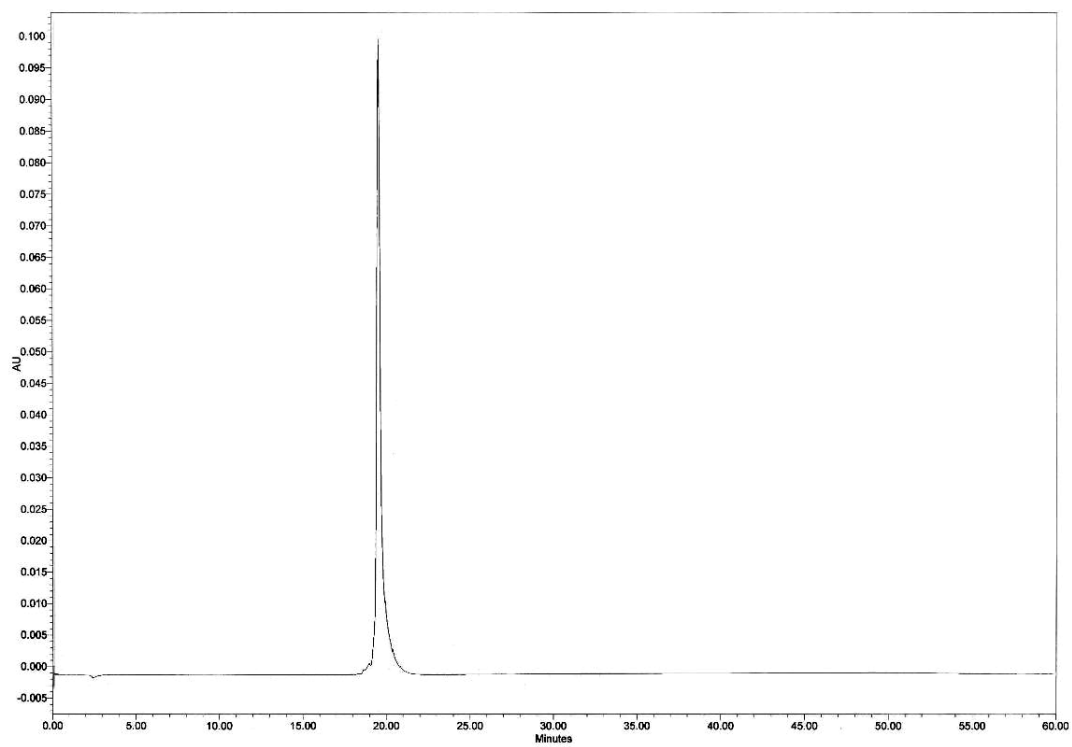


Figure S21. HPLC chromatogram (top) and MALDI-TOF mass spectrum (bottom) of (2'*R*,4'*R*)-pro/(1*S*,2*S*)-acpcPNA Ac-T₇-LysNH₂ (**T7**) (CCA matrix, Reflectron mode) (calcd for $[M+H]^+$: $m/z=2513.2$)

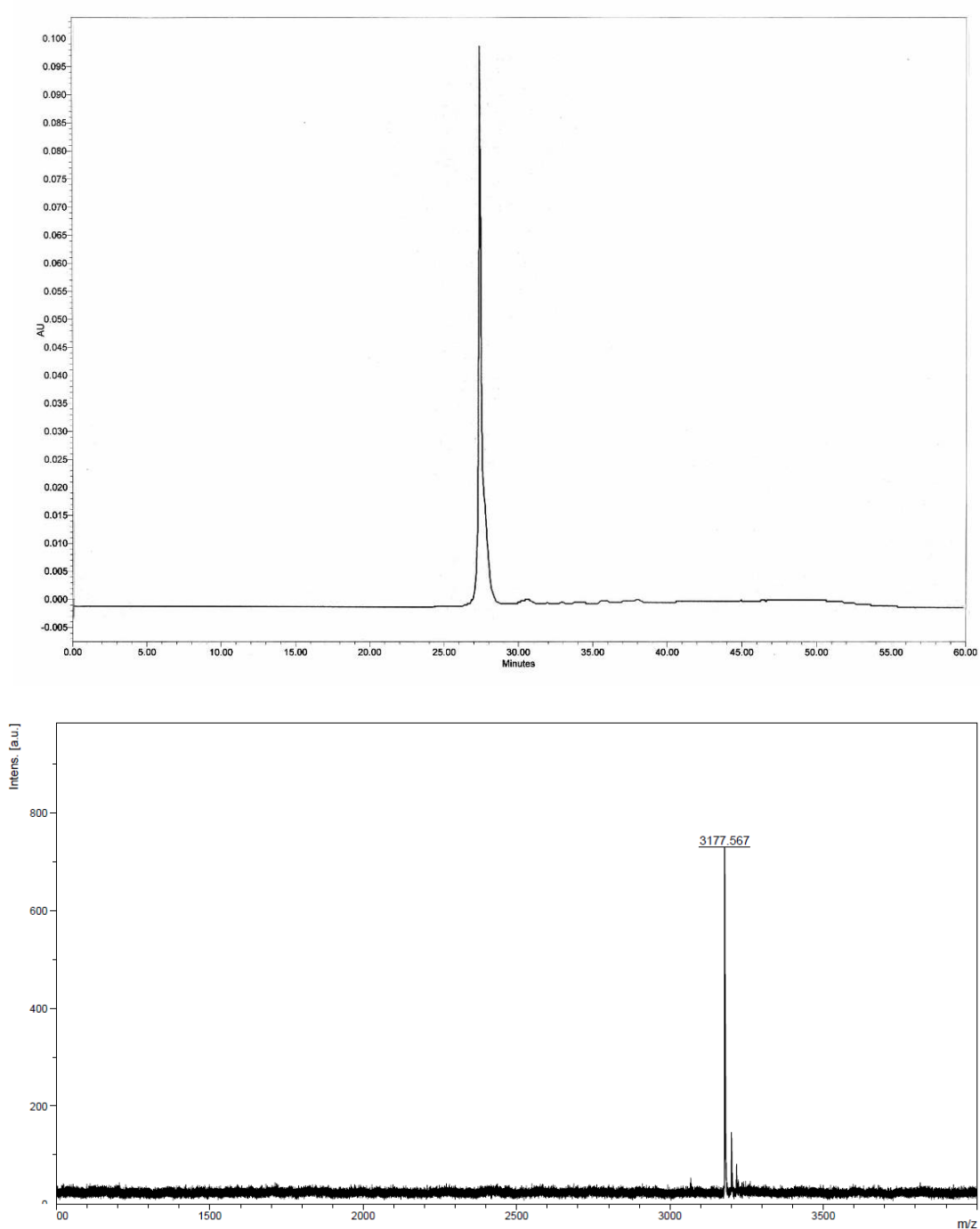


Figure S22. HPLC chromatogram (top) and MALDI-TOF mass spectrum (bottom) of (2'*R*,4'*R*)-pro/(1*S*,2*S*)-acpcPNA Ac-T₉-LysNH₂ (**T9**) (CCA matrix, Reflectron mode) (calcd for $[M+H]^+$: $m/z=3177.5$)

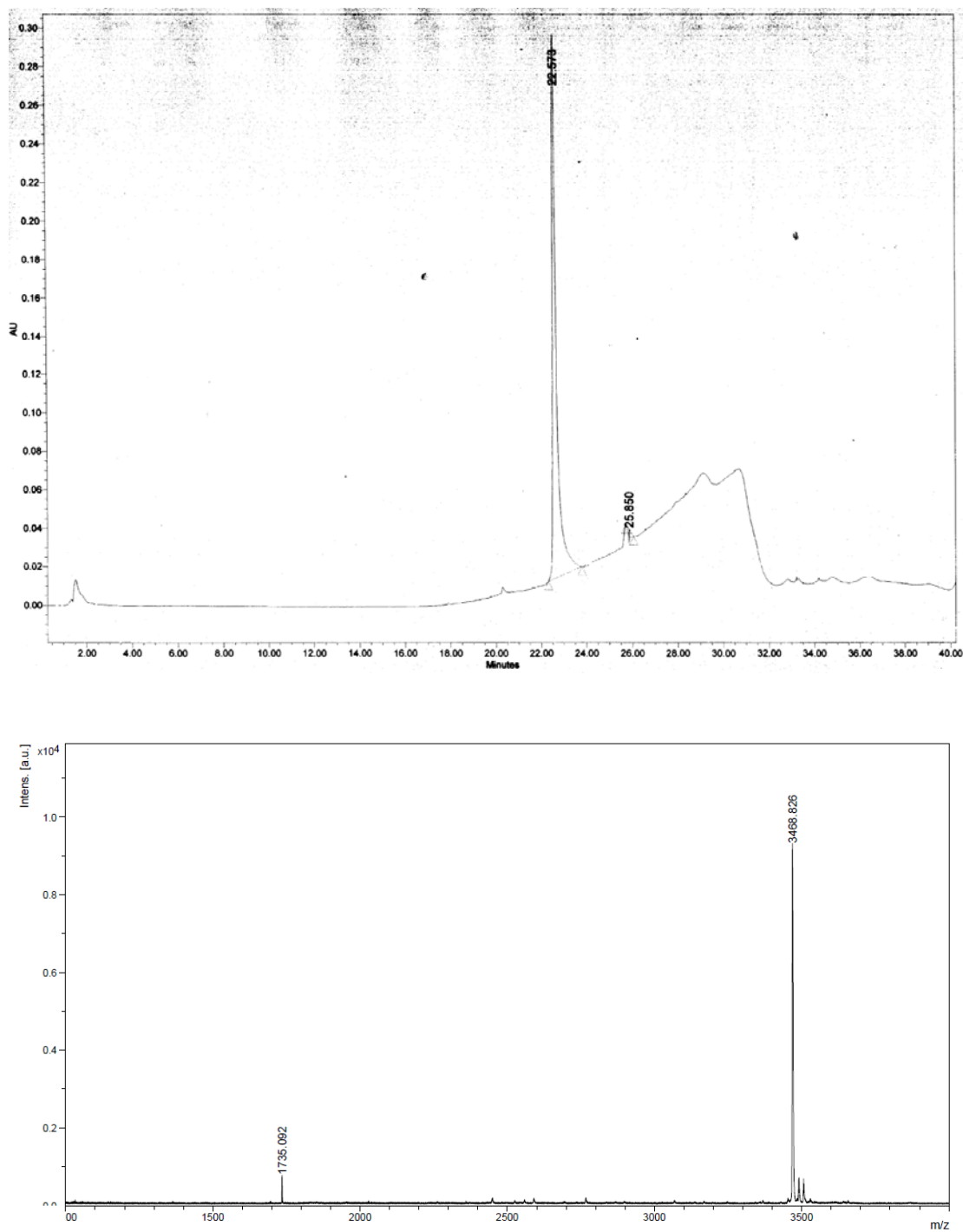


Figure S23. HPLC chromatogram (top) and MALDI-TOF mass spectrum (bottom) of (2'*R*,4'*R*)-pro/(1*S*,2*S*)-acpcPNA H-T₁₀-LysNH₂ (**T10**) (CCA matrix, Reflectron mode) (calcd for $[M+H]^+$: $m/z=3467.6$)

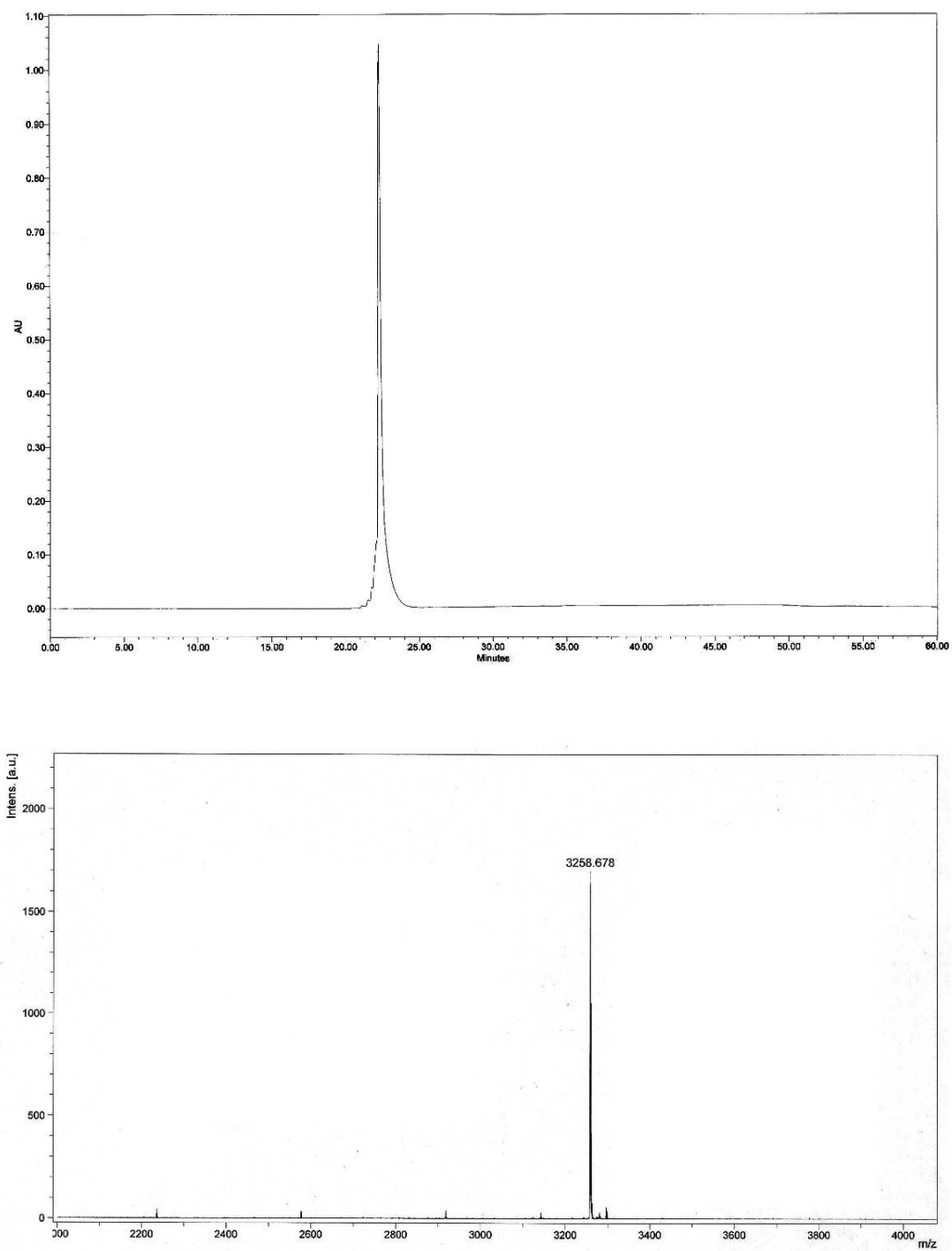


Figure S24. HPLC chromatogram (top) and MALDI-TOF mass spectrum (bottom) of (2'*R*,4'*R*)-pro/(1*S*,2*S*)-acpcPNA Ac-A₉-LysNH₂ (**A9**) (CCA matrix, Reflectron mode) (calcd for $[M+H]^+$: $m/z=3258.6$)

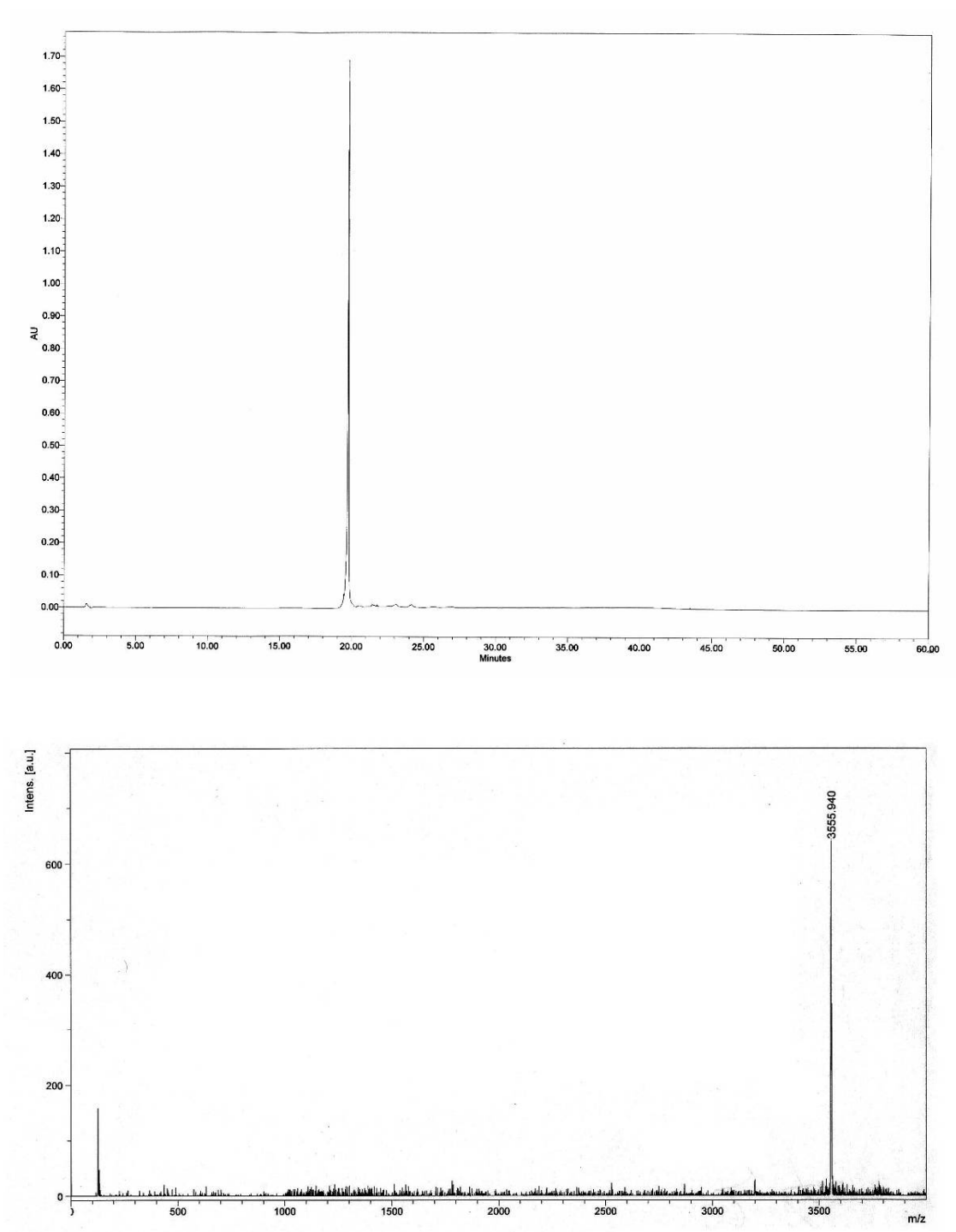


Figure S25. HPLC chromatogram (top) and MALDI-TOF mass spectrum (bottom) of (2'*R*,4'*R*)-pro/(1*S*,2*S*)-acpcPNA Ac-GTAGATCACT-LysNH₂ (**M10a**) (calcd for $[M+H]^+$: $m/z=3556.7$)

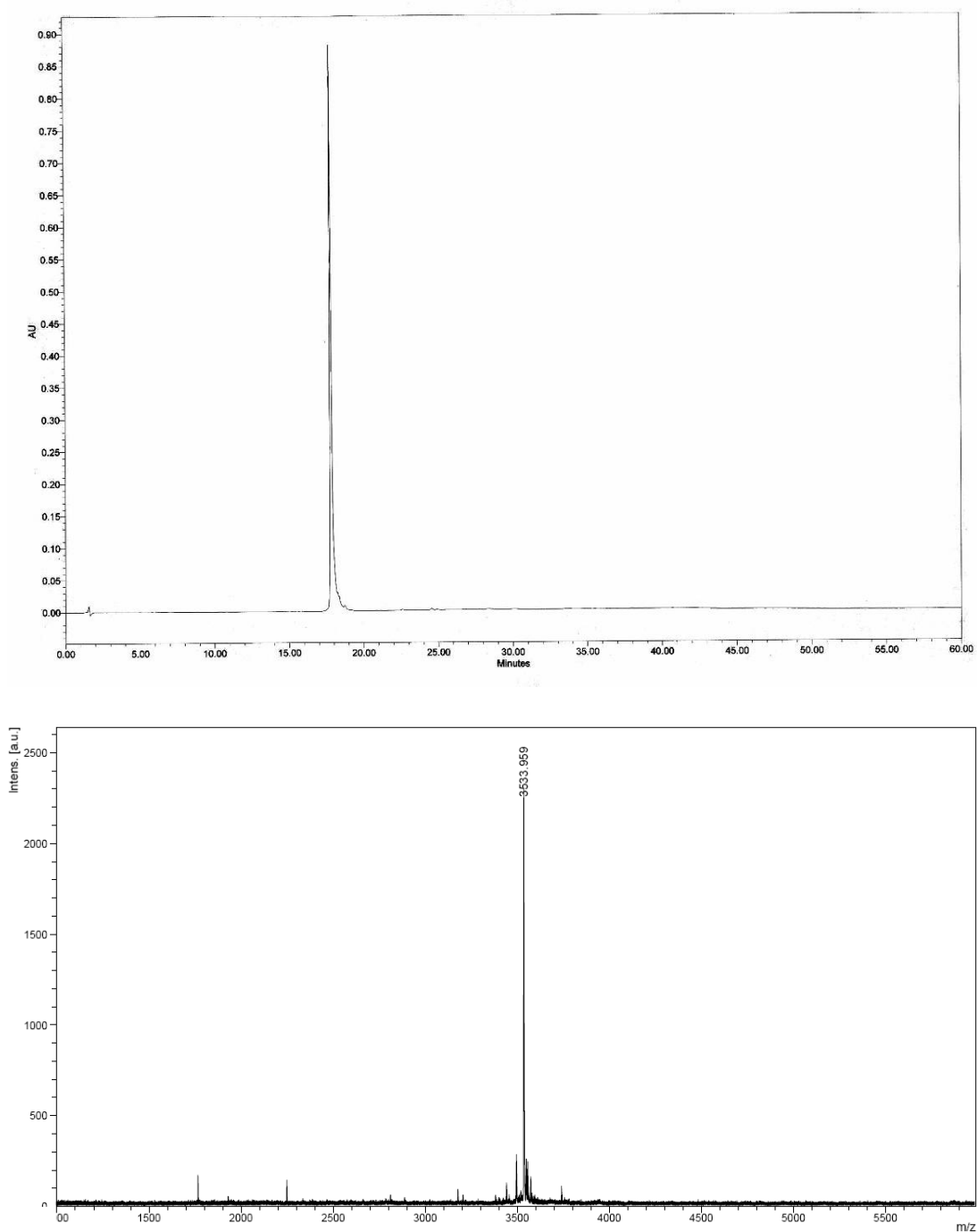


Figure S26. HPLC chromatogram (top) and MALDI-TOF mass spectrum (bottom) of (2'*R*,4'*R*)-pro/(1*S*,2*S*)-acpcPNA Ac- GCTACGTCGC-LysNH₂ (**M10b**) (calcd for $[M+H]^+$: $m/z=3533.7$)

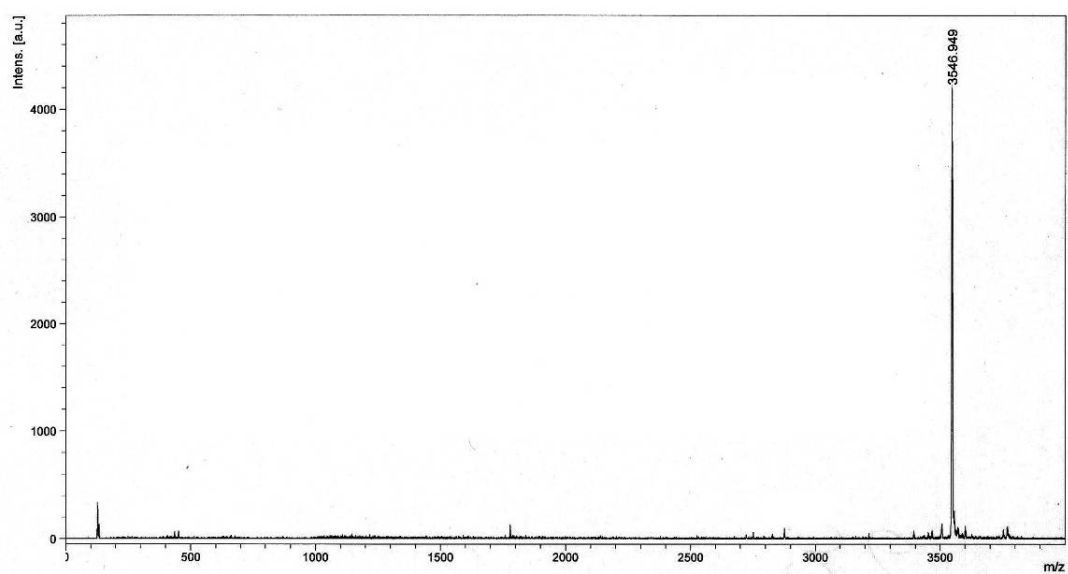
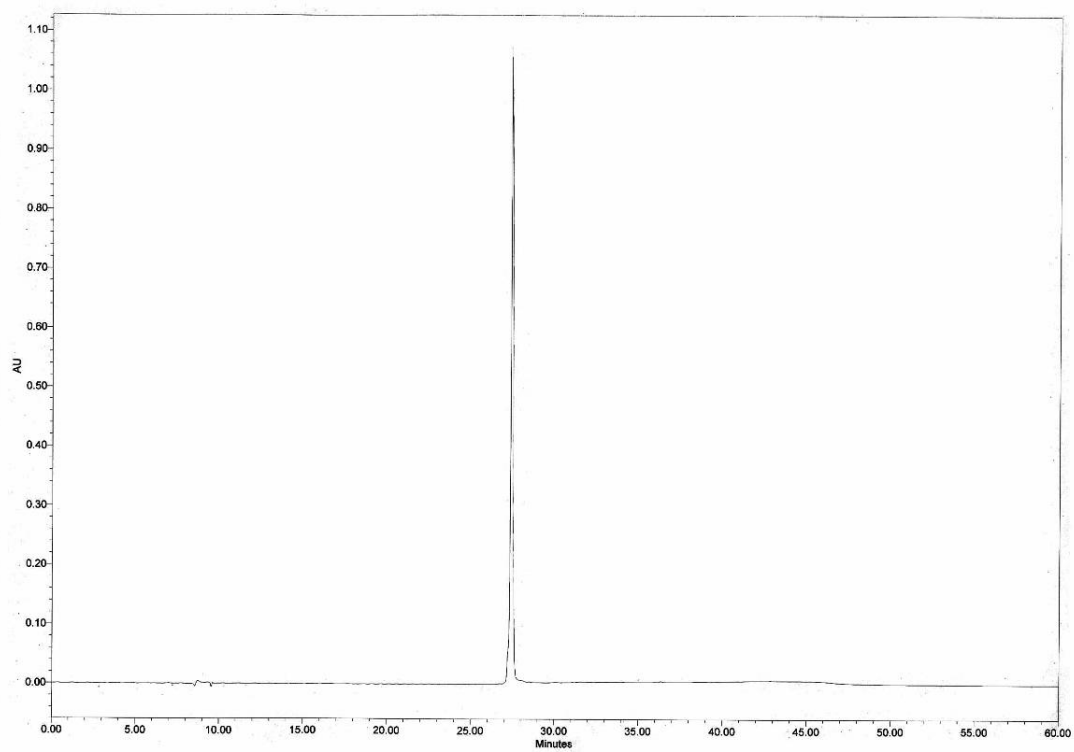


Figure S27. HPLC chromatogram (top) and MALDI-TOF mass spectrum (bottom) of (2'*R*,4'*R*)-pro/(1*S*,2*S*)-acpcPNA Ac-TATGTACTAT-LysNH₂ (**M10c**) (calcd for $[M+H]^+$: $m/z=3546.7$)

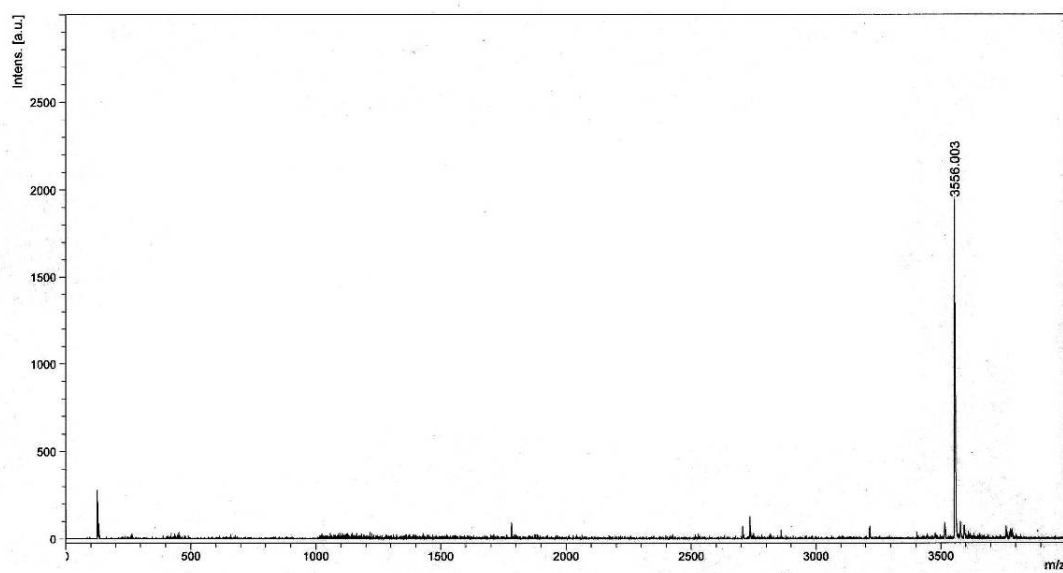
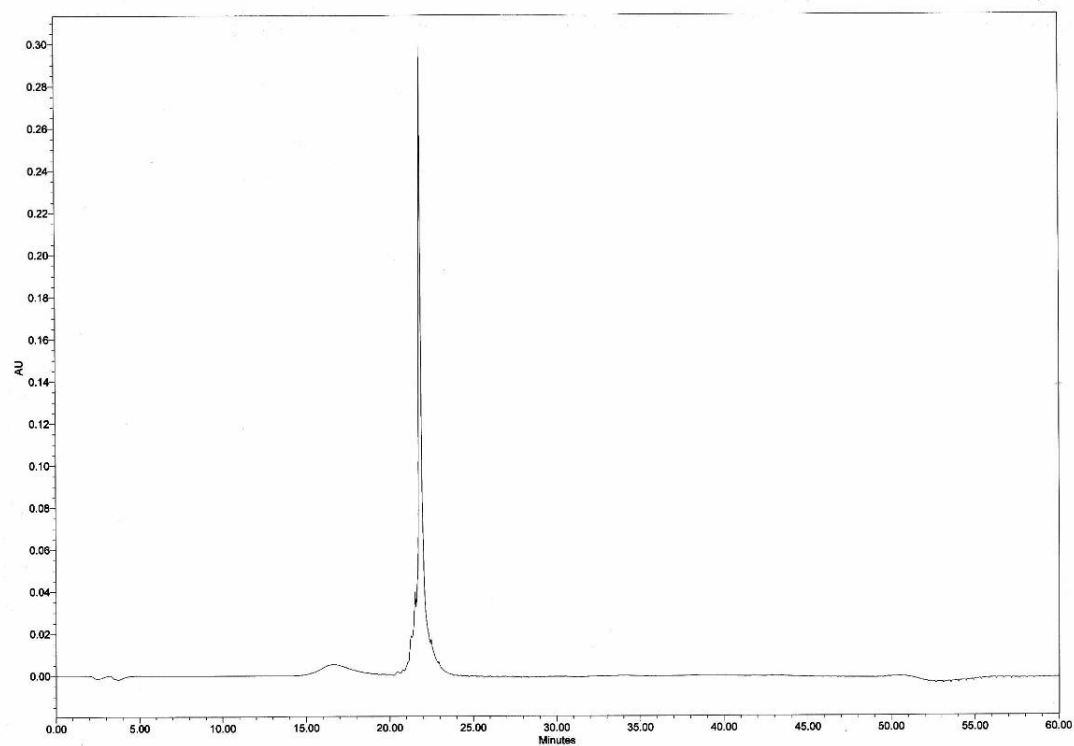


Figure S28. HPLC chromatogram (top) and MALDI-TOF mass spectrum (bottom) of (2'*R*,4'*R*)-pro/(1*S*,2*S*)-acpcPNA Ac-AGTGATCTAC-LysNH₂ (**M10d**) (calcd for $[M+H]^+$: $m/z=3556.7$)

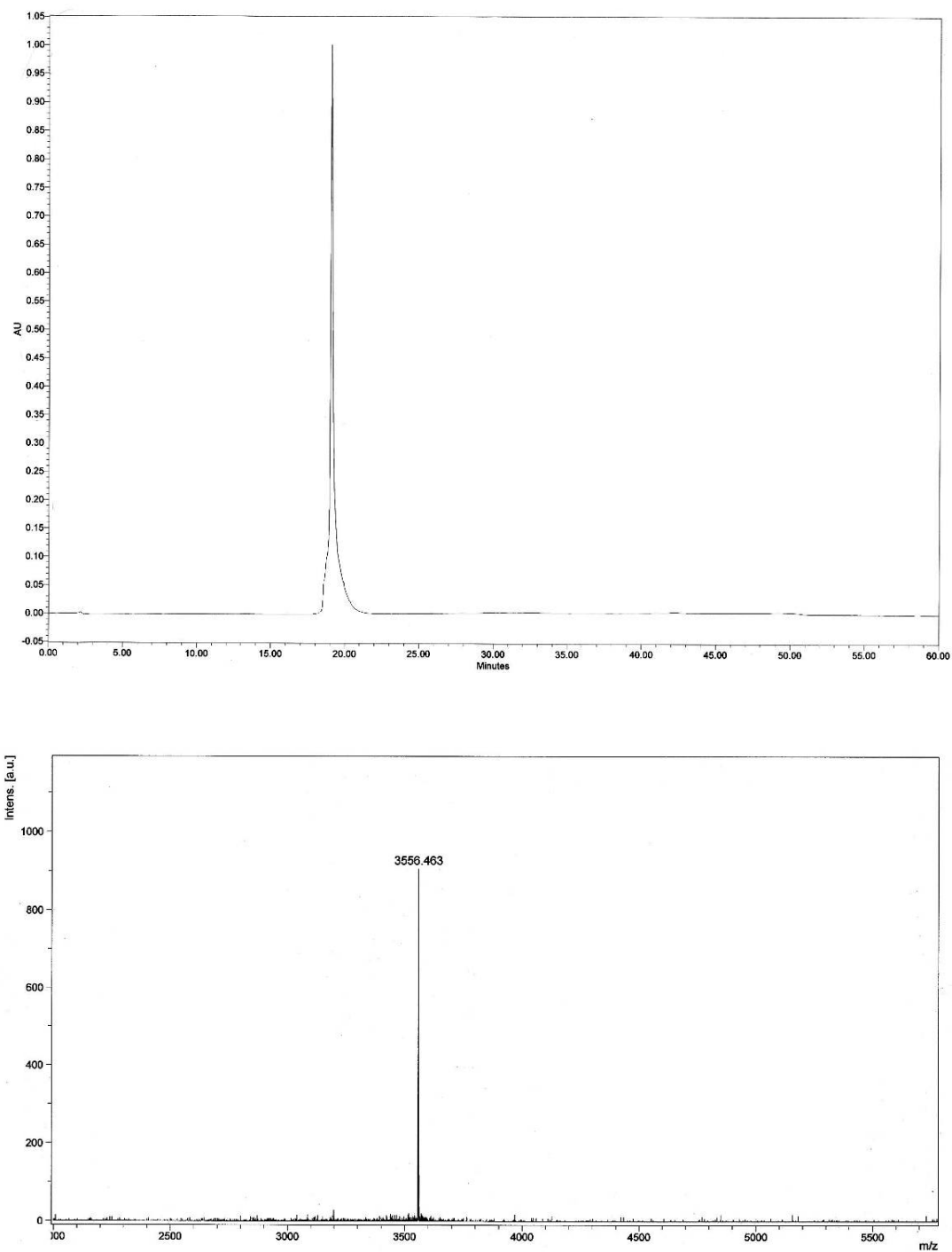


Figure S29. HPLC chromatogram (top) and MALDI-TOF mass spectrum (bottom) of (2'*R*,4'*R*)-pro/(1*S*,2*S*)-acpcPNA Ac-CATCTAGTGA-LysNH₂ (**M10e**) (calcd for $[M+H]^+$: $m/z=3556.7$)

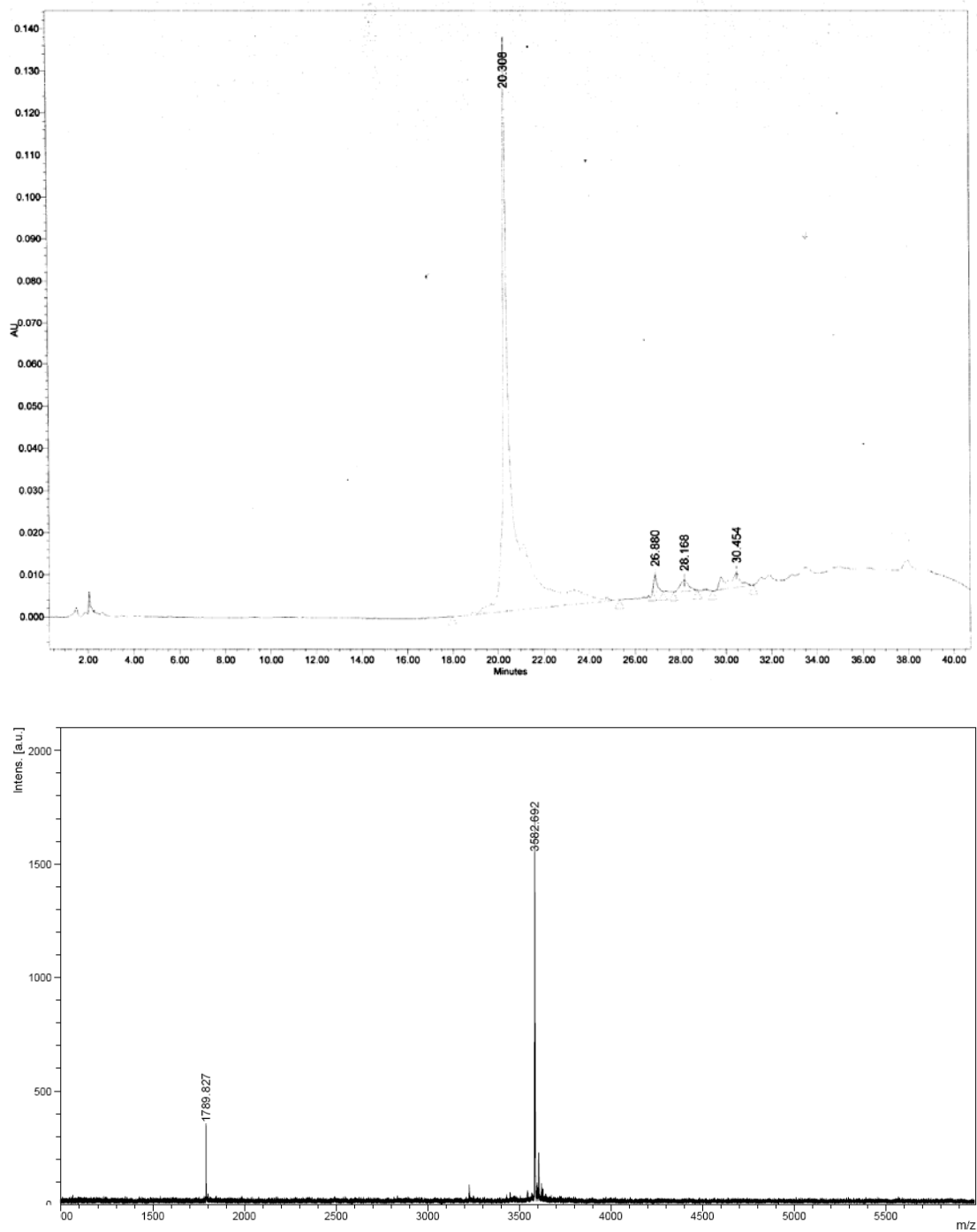


Figure 30. HPLC chromatogram (top) and MALDI-TOF mass spectrum (bottom) of (2'*R*,4'*R*)-pro/(1*S*,2*S*)-acpcPNA Ac-GCGACGTAGC-LysNH₂ (**M10f**) (calcd for [M+H]⁺: $m/z=3582.7$)

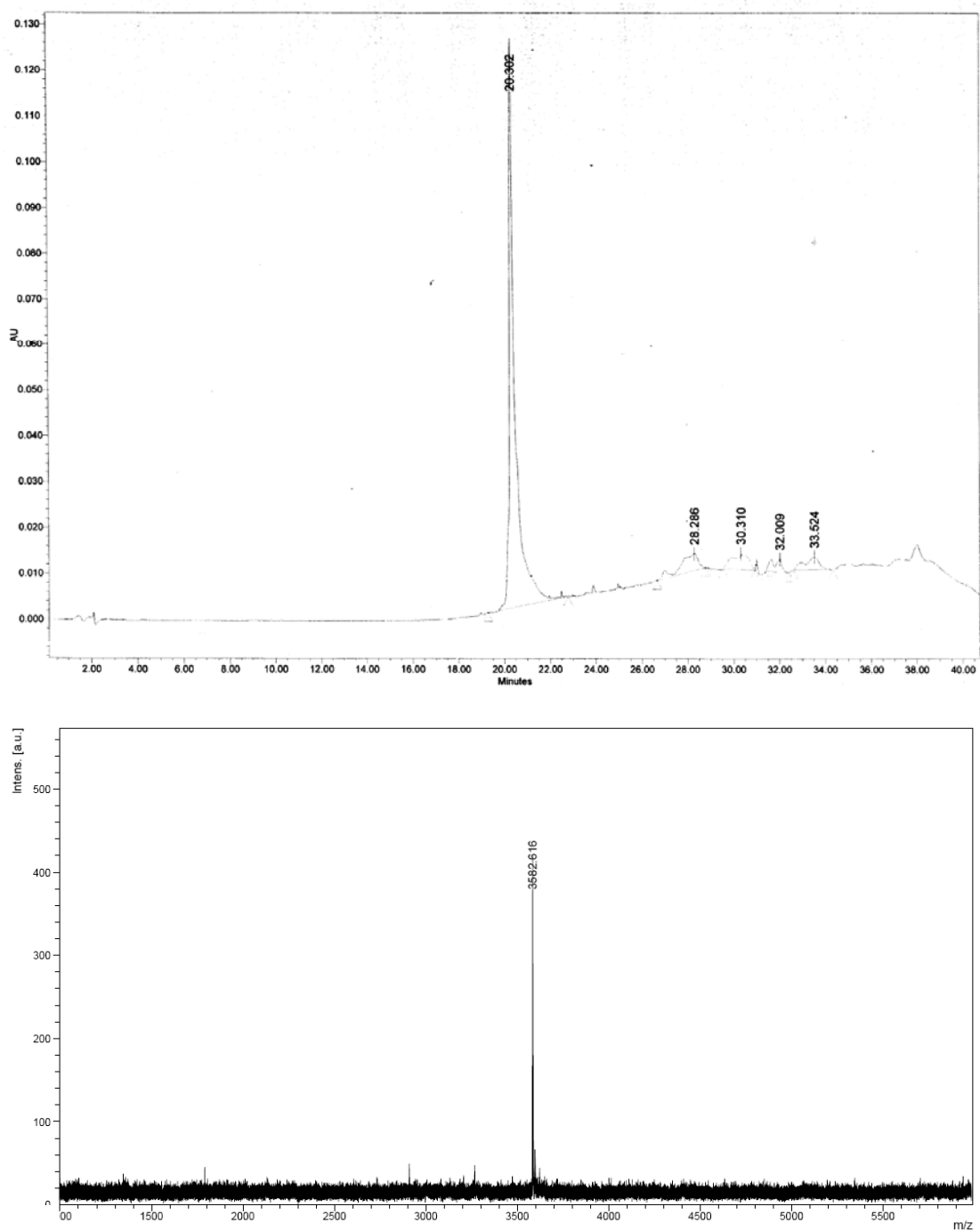


Figure S31. HPLC chromatogram (top) and MALDI-TOF mass spectrum (bottom) of (2'*R*,4'*R*)-pro/(1*S*,2*S*)-acpcPNA Ac-CGATGCAGCG-LysNH₂ (**M10g**) (calcd for [M+H]⁺: *m/z*=3582.7)

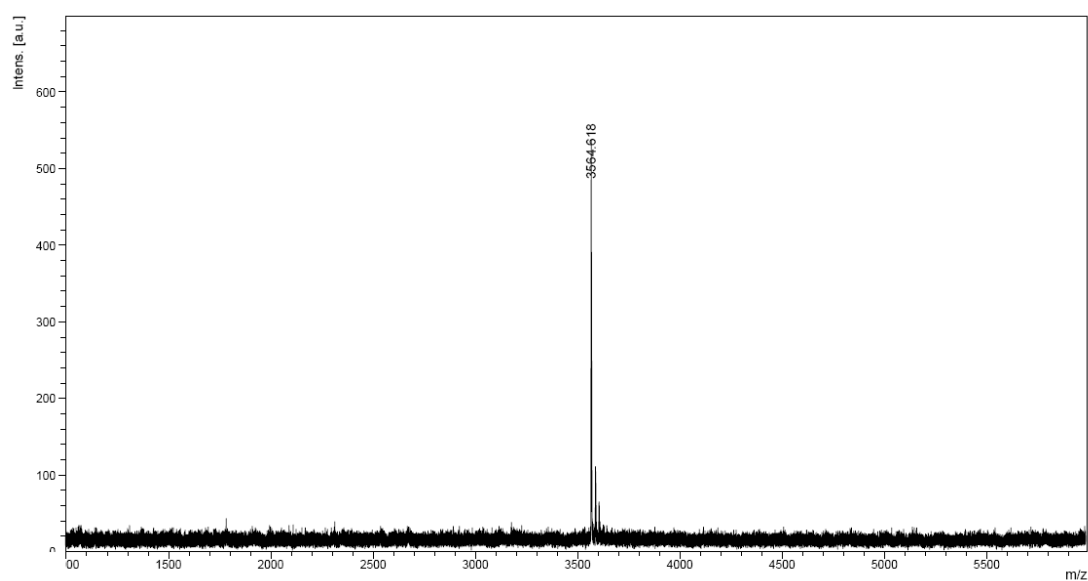
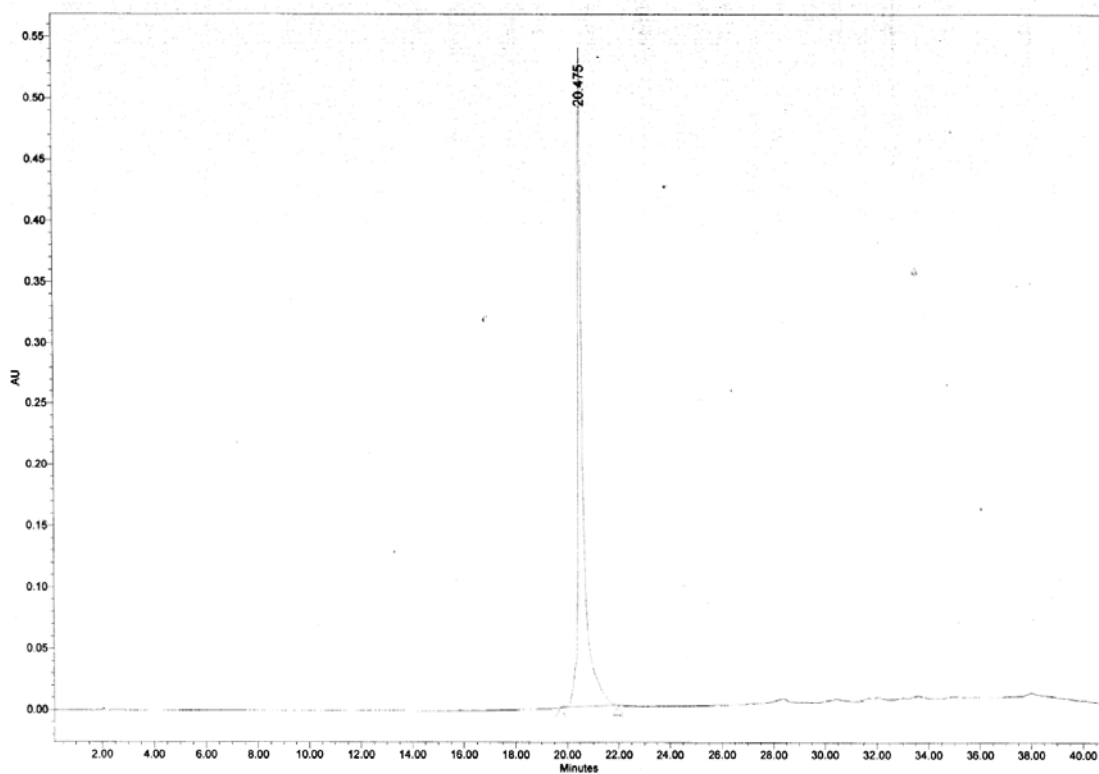


Figure S32. HPLC chromatogram (top) and MALDI-TOF mass spectrum (bottom) of (2'*R*,4'*R*)-pro/(1*S*,2*S*)-acpcPNA Ac-ATAGTACATA-LysNH₂ (**M10h**) (calcd for $[M+H]^+$: $m/z=3564.7$)

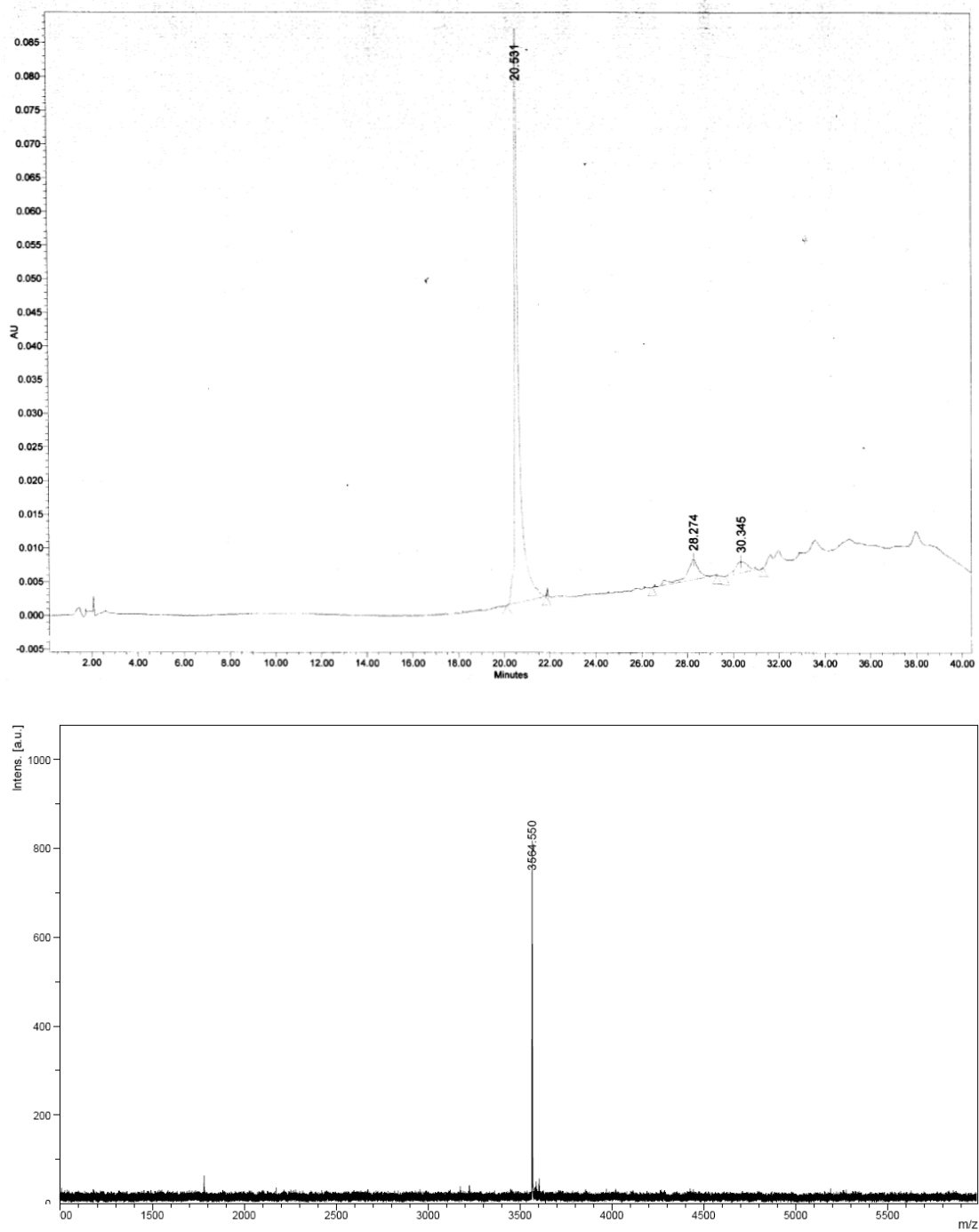


Figure S33. HPLC chromatogram (top) and MALDI-TOF mass spectrum (bottom) of (2'*R*,4'*R*)-pro/(1*S*,2*S*)-acpcPNA Ac-ATACATGATA-LysNH₂ (**M10i**) (calcd for [M+H]⁺: $m/z=3564.7$)

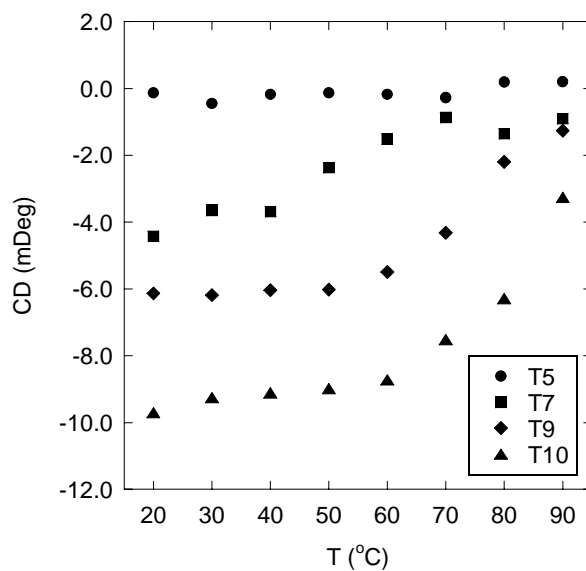


Figure S34. T_m curves of homothymine acpcPNA hybrids: $T_n \cdot dA_n$ obtained from CD experiments (Figure S36). The melting experiments were carried out at concentrations of acpcPNA and DNA of $1.0 \mu\text{M}$ each, and in 10 mM sodium phosphate buffer pH 7.0.

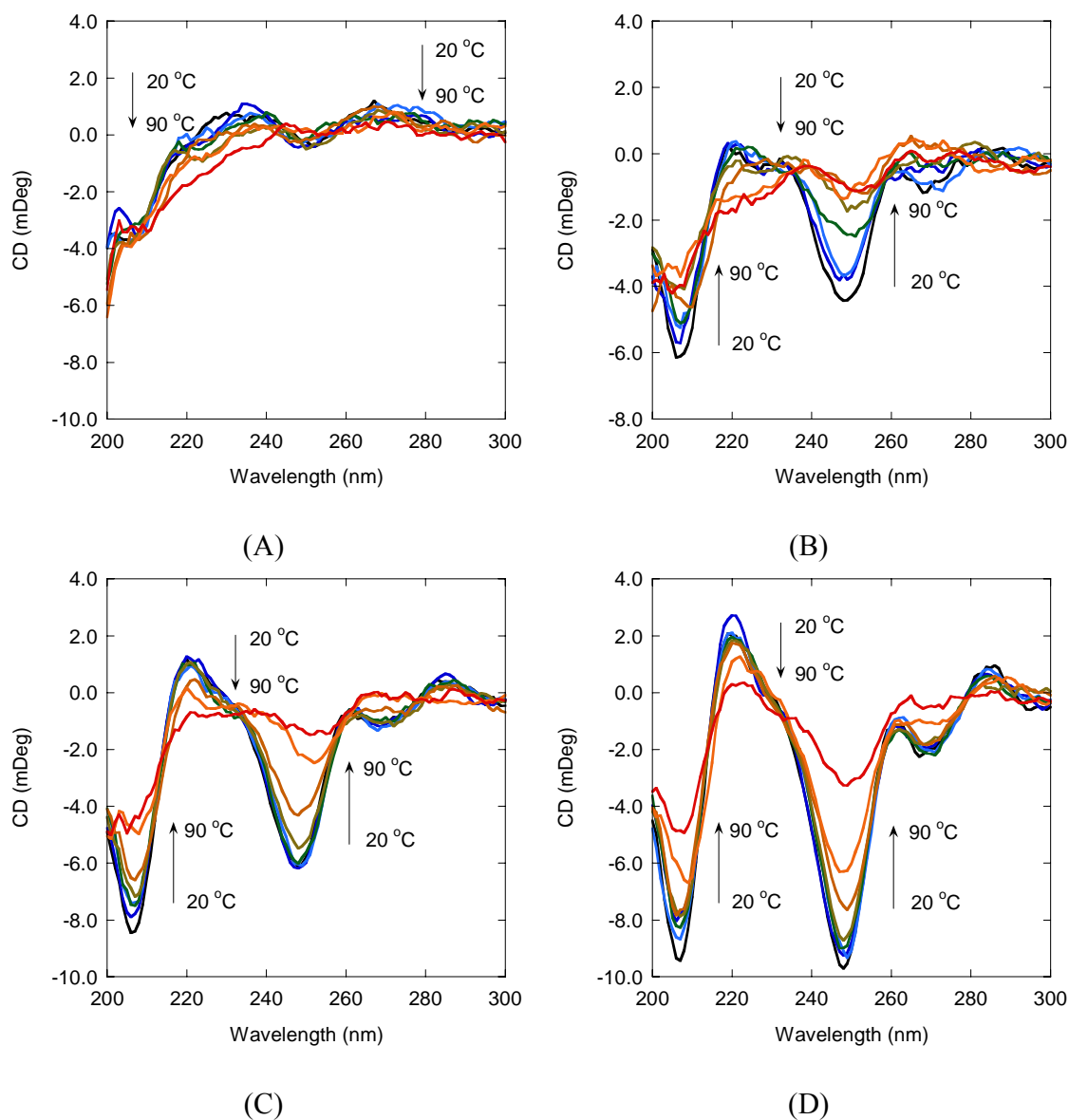


Figure S35. Variable CD spectra of homothymine acpPNA hybrids: **T5**·dA₅ (A) **T7**·dA₇ (B) **T9**·dA₉ (C) and **T10**·dA₁₀ (D). The CD spectra were recorded between 20 – 90 °C concentrations of acpPNA and DNA of 1.0 μ M each, and in 10 mM sodium phosphate buffer pH 7.0.

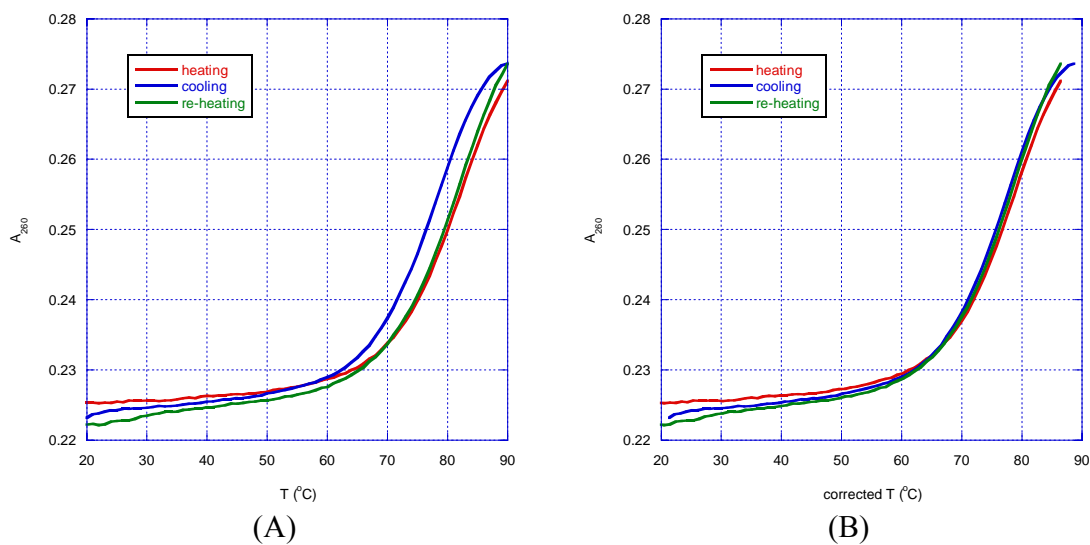


Figure S36. A typical T_m curve obtained from heating, cooling and reheating of the acpPNA·DNA hybrid T7·dA₇ at a heating and cooling rate of 1.0 °C/min and a hold time at the end of each cycle of 10 min, without (A) and with (B) temperature correction. The melting experiment was performed at concentrations of acpPNA and DNA of 1.0 μ M each, and in 10 mM sodium phosphate buffer pH 7.0.

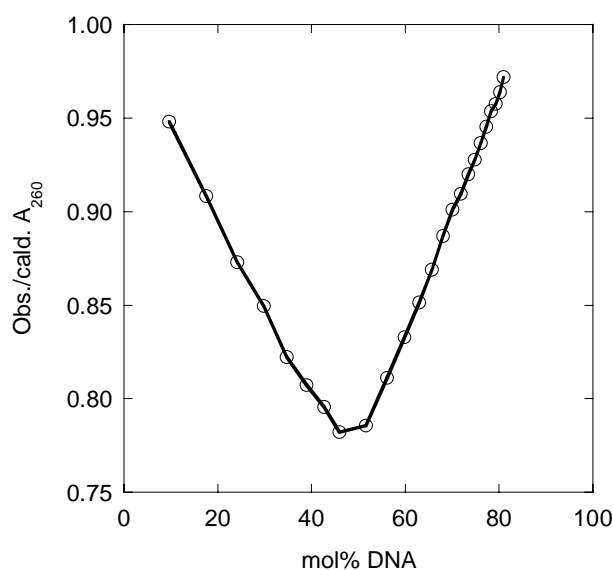


Figure S37. UV titration curve of acpcPNA **T9** (analyte) (initial concentration=2.3 μM) with DNA dT₉ (38.5 μM) as titrant. The titration was carried out in 10 mM sodium phosphate pH 7.0 containing 100 mM NaCl at 25 °C. The plot shows the ratio of observed/calculated A₂₆₀ after each addition.³ The UV titration revealed one inflection point at the acpcPNA:DNA ratio of 1:1.

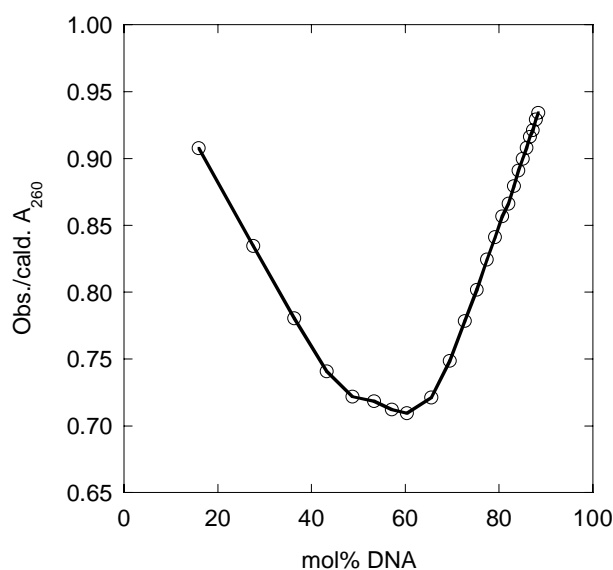
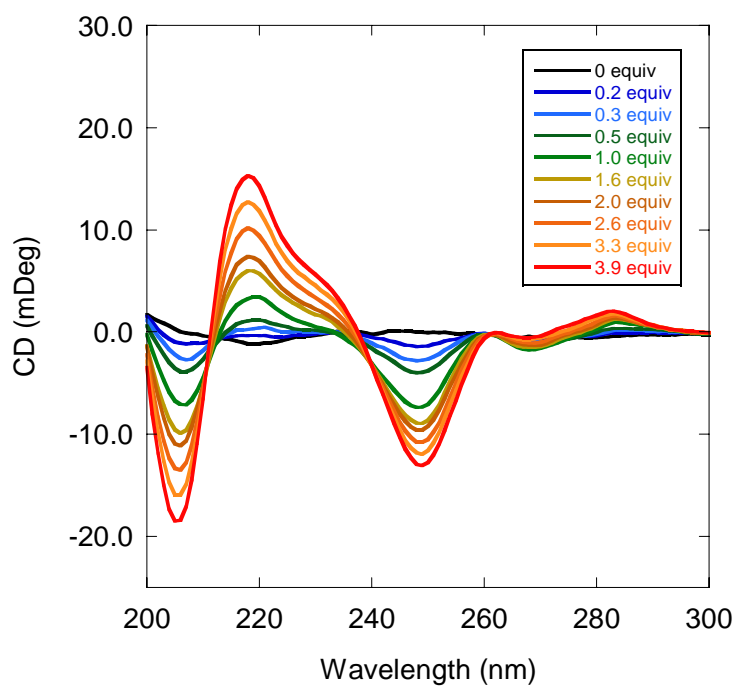
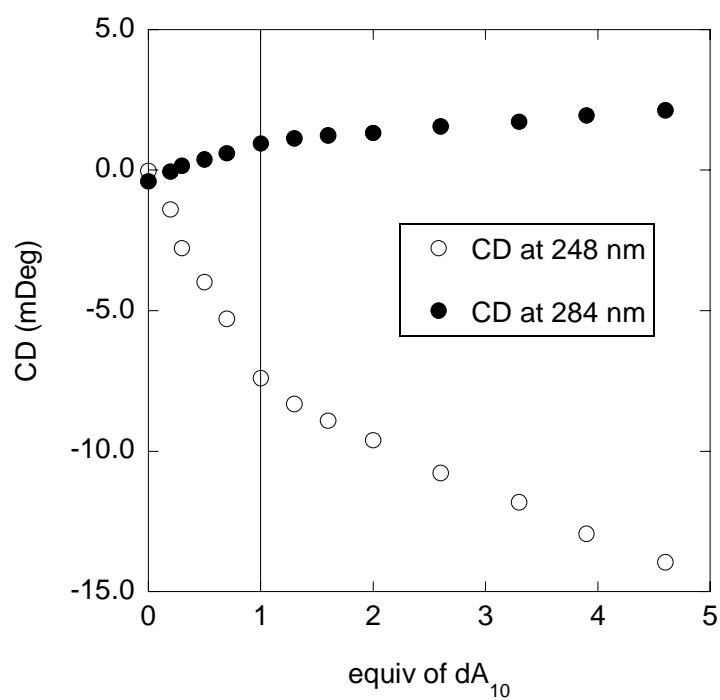


Figure S38. UV titration curve of acpcPNA **A9** (analyte) (initial concentration=1.3 μM) with DNA dT₉ (39.4 μM) as titrant. The titration was carried out in 10 mM sodium phosphate pH 7.0 containing 100 mM NaCl at 25 °C. The plot shows the ratio of observed/calculated A₂₆₀ after each addition.³ The UV titration revealed two inflection points at acpcPNA:DNA ratio of 1:1 and 1:2 respectively.



(A)



(B)

Figure S39. CD spectra (A) and CD titration curves at 248 and 284 nm (B) of acpcPNA T10 (analyte) (initial concentration = 1.1 μM) with dA₁₀ (173.0 μM) as titrant. The titration was carried out in 10 mM sodium phosphate pH 7.0 at 25 $^{\circ}\text{C}$.

References:

1. Vilaivan T, Srisuwannaket C. Hybridization of pyrrolidinyl peptide nucleic acids and DNA: Selectivity, base-pairing specificity, and direction of binding. *Org Lett* 2006; 8:1897–900.
2. Lowe G, Vilaivan T. Dipeptides bearing nucleobases for synthesis of novel peptide nucleic acids. *J Chem Soc Perkin Trans 1* 1997; 547–54.
3. Vilaivan T, Lowe G. A novel pyrrolidinyl PNA showing high sequence specificity and preferential binding to DNA over RNA. *J Am Chem Soc* 2002; 124:9326–7.